Geophys. J. Int. (2000) **142,** 783–800

A reappraisal of postglacial decay times from Richmond Gulf and James Bay, Canada

J. X. Mitrovica[1], A. M. Forte[2] and M. Simons[3]

[1] *Department of Physics, University of Toronto, Toronto, Ontario, Canada. E-mail: jxm@physics.utoronto.ca*
[2] *Department of Earth Sciences, University of Western Ontario, London, Ontario, Canada*
[3] *Seismological Laboratory, California Institute of Technology, Pasadena, CA, USA*

Accepted 2000 March 30. Received 2000 March 10; in original form 1999 October 15

SUMMARY

Decay times inferred from relative sea-level (RSL) histories of previously glaciated regions provide a potentially important constraint on mantle rheology. We present a new compilation of RSL data from Richmond Gulf and James Bay, Canada. This recompilation reveals errors in previous compilations that led to inaccurate estimates for the Richmond Gulf decay time in a series of recently published articles. We derive updated estimates for the decay time at Richmond Gulf and James Bay using a methodology that incorporates errors in both the age and the height of the sea-level markers. This exercise is guided by a series of synthetic RSL calculations that show that decay time estimates in the region can be significantly biased if the RSL time-series are not corrected for global eustatic sea-level trends, or if the estimates are based on composite RSL histories derived by combining data from both the Richmond Gulf and the James Bay regions. Our decay time analysis for Richmond Gulf applies the pioneering approach of Walcott (1980) to a large database and we derive a value of 4.0–6.6 kyr, where the range is defined by a misfit tolerance 10 per cent higher than the minimum. Our analysis for James Bay is based on the uplift curve derived by Hardy (1976), and we estimate a decay time of about 2.0–2.8 kyr. The difference between our estimates for Richmond Gulf and James Bay may be due to errors in the observational record from these regions, but could also be influenced by lateral variations in lithospheric structure associated with the assembly of Laurentia.

Key words: glacial rebound, Hudson Bay, mantle viscosity, sea level.

1 INTRODUCTION

Inferences of mantle viscosity based on data associated with glacial isostatic adjustment are complicated by their sensitivity to both mantle rheology and the space–time history of Late Pleistocene and Holocene ice cover. Various approaches have been developed to deal with this complexity. As an example, one approach is to converge towards a global ice and earth model combination via an analysis of widely distributed relative sea-level (RSL) histories (e.g. Wu & Peltier 1983; Tushingham & Peltier 1991, 1992). The disadvantage of this approach is that ice models thus derived are inextricably linked to a specific earth model, and they are therefore of limited utility in independent studies of mantle viscosity. A similar approach has been applied to regional as opposed to global ice models (e.g. Lambeck 1993; Lambeck *et al.* 1998).

An independent approach to the mantle viscosity problem involves the determination of RSL data parametrizations that are insensitive to ice histories. An example is the so-called Fennoscandian relaxation spectrum (FRS) (McConnell 1968). McConnell (1968) used uplifted beach records along a $\sim$1000 km profile of the Fennoscandian region to determine the postglacial decay time as a function of the wavelength of the deformation. The FRS is, at least in theory, independent of the surface loading. As a second example, Nakada & Lambeck (1989) inferred a radial viscosity profile using differential sea-level highstands at pairs of sites in the far field of the major Late Pleistocene ice complexes. Sea level trends at such sites (e.g. Australia) are characterized by episodes of sea-level rise during the major deglaciation phase followed by a gradual sea-level fall over the Late Holocene. The amplitude of the associated highstand may be sensitive to relatively minor melting beyond the main deglaciation event; however, this sensitivity is removed if a simple difference between highstands at relatively nearby sites is adopted in the inference procedure. Most recently, Mitrovica has advocated the use of site-specific postglacial decay (or relaxation) times (e.g. Mitrovica & Forte 1997). RSL curves obtained from previously glaciated regions are

characterized by simple exponential-like forms (Andrews 1970; Walcott 1980). The decay time that governs this model form is relatively insensitive to details of the ice load history (Mitrovica & Peltier 1995).

Unfortunately, estimates of decay times for sites in Hudson Bay have varied dramatically (see below), and the robustness of several previous inferences of mantle viscosity has recently been called into question (Peltier 1998). We present a detailed re-appraisal of postglacial decay times in Hudson Bay using the available RSL data set. Our primary goal is to derive rigorous bounds on these decay times that reflect the quality of the existing observational constraints.

2 BACKGROUND

The first estimations of postglacial relaxation times for Hudson Bay can be traced to Andrews (1970) and Walcott (1972, 1980). Following Andrews (1970), we introduce a simple exponential form for the sea-level change remaining at some time t during the deglaciation phase (SL):

$$\mathrm{SL}(t) = A \exp(-t/\tau). \tag{1}$$

To simplify later discussion, we will assume that $t=0$ is the present [rather than the onset of deglaciation used by Andrews (1970)]. Andrews (1970) adopted eq. (1) as a model for postglacial uplift curves determined by survey and estimated a decay time, τ, of roughly 2000 years.

Andrews' (1970) estimate of the relaxation time has played an influential role in studies of glacial isostatic adjustment. The shortness of the decay time, relative to the period elapsed since the end of deglaciation, suggests that the uplift remaining in Hudson Bay is small; however, this conclusion appears to be inconsistent with the observation of a relatively large free-air gravity anomaly over the region (Kaula 1972; Walcott 1973; Cathles 1975; Simons & Hager 1997). This inconsistency led to a suggestion by Peltier and co-workers that the remnant adjustment of Hudson Bay is controlled by a far longer relaxation time associated with the deformation of the 670 km seismic discontinuity (Peltier & Wu 1982; Peltier 1982, 1985; Wu & Peltier 1983); however, subsequent work has shown that the contribution from this process to the present-day gravity field would be far too small in this regard. Most recent studies suggest that the observed anomaly originates from some combination of a rebound and mantle convection signature (Peltier *et al.* 1992; Forte & Mitrovica 1996; Pari & Peltier 1996; Simons & Hager 1997). Alternatively, the relaxation time inferred by Andrews (1970) may be either inaccurate (that is, the sea-level data upon which it was based may be suspect) or inappropriate for the entire Laurentide platform.

The procedure for estimating the relaxation time used in Andrews (1970) is not strictly valid, since observational data are relative measures of sea level (that is, only the sea-level change between some time t and the present is known). Indeed, a more appropriate model for RSL data is

$$\mathrm{RSL}(t) = \mathrm{SL}(t) - \mathrm{SL}(0) = A\{\exp(-t/\tau) - 1\}, \tag{2}$$

which ensures that the simple model for the observations passes through zero at present ($t=0$). Eq. (2) makes it clear, as suggested by Walcott (1980, p. 6), that '[the] technique of estimating relaxation times by plotting the log of the uplift against time will work only if the remaining uplift is small'. That is, the approach used by Andrews (1970) is valid only if the value A (the sea-level change remaining at the present day) is small relative to the value SL(t) for any datum on the RSL curve.

Walcott (1980) actually fitted a slightly modified form of eq. (2) through the RSL curve. In particular, he argued that the exponential curve need not go precisely through zero at the present day 'because of the uncertainty in absolute height and age' (p. 7). As we will discuss below, Walcott (1980) established a sea-level curve in the Richmond Gulf region of Hudson Bay using a consistent set of shell samples. He argued in this respect that 'intervals of height and age between any two samples are better determined than the absolute height and age of any one sample [and] the position of sea level relative to the beach at the time the shells were placed in the beach is not known and further the age of the shell material when the mollusc was living is uncertain' (Walcott 1980, p. 7). Effectively, he found the range of acceptable τ values by fitting the equation

$$\mathrm{RSL}(t) = A\{\exp(-t/\tau) - 1\} + c \tag{3}$$

through RSL data collected at Richmond Gulf and Castle Island in 'southeastern Hudson Bay' (see Fig. 1). Walcott (1980) arrived at two important conclusions. First, the postglacial relaxation time for this region has a lower bound of $\sim$5000 years. Second, this relaxation time, associated with sites near the centre of the uplifting Laurentide region (where the peak free-air gravity anomaly is obtained) is longer than the relaxation times that characterize the postglacial uplift of 'edge' sites [which cluster close to the value of 2000 years estimated by Andrews (1970)].

Mitrovica & Peltier (1993) revisited the Hudson Bay relaxation time question using RSL data from three sites in the Tushingham & Peltier (1991) database of sea-level histories: Southampton Island, Ungava Peninsula and Ottawa Island (see Fig. 1). They found that the first two of these sites, in northern Hudson Bay, are characterized by postglacial relaxation times of 3.3 and 2.0 kyr, respectively. Ottawa Island is located near the centre of the rebounding region. The RSL curve published by Tushingham & Peltier (1991) for this site is based on data from Andrews & Falconer (1969). Mitrovica & Peltier (1993) estimated a decay time of 2.5 kyr for Ottawa Island, which disagrees with the minimum bound of 5 kyr derived by Walcott (1980) for the same central region (Richmond Gulf, Castle Island). Walcott (1980) was aware that the Andrews & Falconer (1969) database yielded a relatively short decay time, and he argued that the inconsistency with his result for Richmond Gulf 'lies in the [quality of the] Ottawa Island data' (p. 6).

The decay time for Richmond Gulf remains a source of significant interest. Peltier (1994) computed a relaxation time of 7.6 kyr for the site on the basis of data from Hillaire-Marcel (1980), as cited in the Tushingham & Peltier (1991) database. Mitrovica & Peltier (1995) also used the Tushingham & Peltier (1991) database and arrived at the same result for the site. Furthermore, Simons & Hager (1997) used the decay time of 7.6 kyr for Richmond Gulf as an *a posteriori* check on a viscosity model derived on the basis of a spatio–spectral analysis of the free-air gravity field over Hudson Bay. However, they recognized, following the analysis by Mitrovica & Forte (1997), that 'sea-level records in [Hudson Bay] indicate a spread of relaxation times' (Simons & Hager 1997, p. 503).

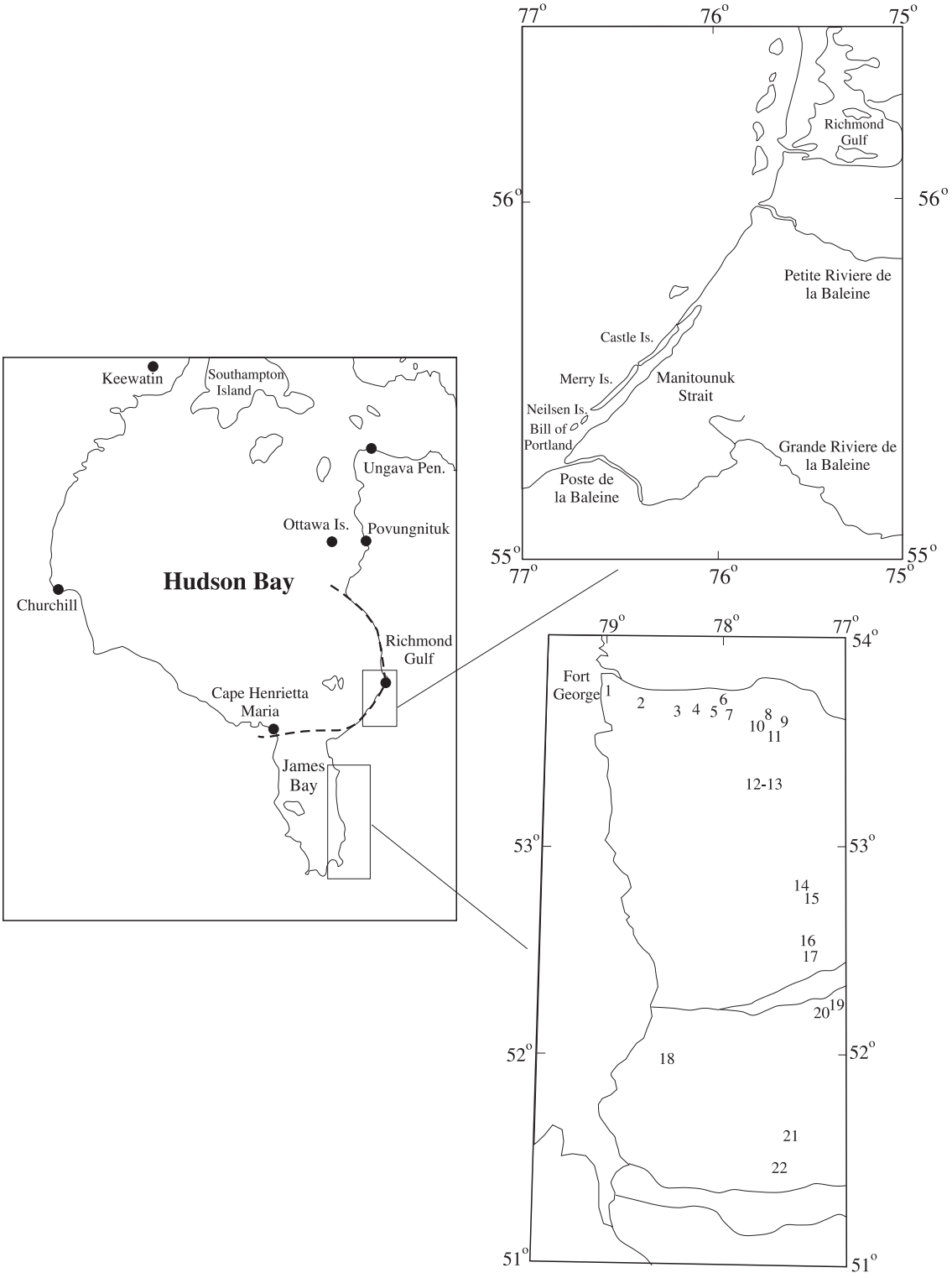

Figure 1. Location maps for the various sites in Hudson Bay referred to in the text. The two maps on the right show details of the Richmond Gulf and eastern James Bay regions. The former is adapted from Hillaire-Marcel (1976), while the latter is revised from Hardy (1976). The numbers 1–22 on the James Bay inset provide the locations for sites in the Hardy (1976) database (see Table 1). The dashed line on the main figure shows the approximate location of the contact between the Belcher Belt to the west and the Superior Province to the east (see text for details).

Mitrovica & Peltier (1995) extended earlier work to estimate decay times at five sites in addition to Richmond Gulf: James Bay (1.5 kyr), Cape Henrietta Maria (greater than $\sim$13 kyr), Ottawa Island (2.5 kyr), Southampton Island (4.9 kyr) and Ungava Peninsula (2.0 kyr). They noted that many of the sea-level curves in the Tushingham & Peltier (1991) database are 'trends' established via subjective extrapolation of relatively sparse age–height pairs obtained by survey. They eschewed such curves [which include entries in the Tushingham & Peltier (1991) database for all five sites listed above, but not Richmond

Gulf] in favour of the data cited in original references [e.g. Hardy (1976, 1977) for James Bay, Andrews & Falconer (1969) for Ottawa Island, Webber *et al.* (1970) for Cape Henrietta Maria, Mathews (1966) for Ungava Peninsula and Walcott (1972) for a suite of sites]. This range of relaxation times lead Mitrovica & Peltier (1995) to question the accuracy of the Hudson Bay database of RSL histories.

Peltier (1996) and Mitrovica & Forte (1997) analysed RSL data from a large number of sites in Laurentia and Arctic Canada, and inferred a wide range of decay times. Mitrovica & Forte (1997) concluded that these decay times cannot be reconciled by a single (radially stratified) earth model and, accordingly, their inversions for viscosity yielded intermediate decay times ($\sim$3.3–3.8 kyr) for the region.

Peltier (1998) argued, in a re-examination of available RSL histories in 'southeastern' Hudson Bay, for a consistent decay time of $\sim$3.4 kyr for the entire region (including Richmond Gulf and James Bay). The analysis raises two questions. First, Peltier (1998) estimated the decay time of the region from a 'composite [RSL] record based on samples collected over a broad spatial area' (p. 607) stretching roughly 600 km. No new RSL samples were used by Peltier (1998) and therefore it is unclear whether his procedure does not simply obscure decay time variations evident in earlier site-specific analysis. Second, Peltier (1998) claimed that the 7.6 kyr decay time frequently cited for Richmond Gulf is inaccurate.

We re-examine the available set of RSL data from Hudson Bay, including all age–height pairs used in previous analyses. The re-analysis serves several purposes. First, we provide an updated compilation of these data that corrects and extends previous tabulations. Second, using an extended Monte Carlo procedure we determine acceptable ranges for postglacial decay times at specific sites for future use by others. Third, we present synthetic calculations that examine the influence of various assumptions and simplifications adopted in previous decay time analyses. Finally, we will consider the implications of our new results for previous inferences of mantle viscosity.

3 HILLAIRE-MARCEL (1980) AND THE RICHMOND GULF DECAY TIME

Recent efforts to estimate the characteristic decay time for Richmond Gulf have generally been based on the RSL constraints provided by Hillaire-Marcel (1980). In Fig. 2(a) we reproduce Fig. 6 of that publication (the only exception is that our ordinate axis, labelled 'Relative Sea Level', appears as 'Elevation' in the original publication). The small crosses on the figure represent RSL constraints obtained by assuming that a 45 yr cycle governs the formation of beach ridges (Hillaire-Marcel & Fairbridge 1976). That is, in this case the sidereal ages of the beaches are determined by simply counting the appropriate number of cycles. The ages quoted by Hillaire-Marcel (1980) for these data clearly represent sidereal ages (note the abscissa label he adopted). The dimensions of the individual crosses do not reflect uncertainties in either height or age; they are merely adopted as shown from the original publication.

The solid dots in the figure represent actual age–height pairs determined by survey and compiled by Hillaire-Marcel (1976, 1980). These data were collected from three sites in close proximity (see Fig. 1 and the discussion below): Castle Island (ages 1.79 and 3.36 kyr), Petite Riviere de la Baleine

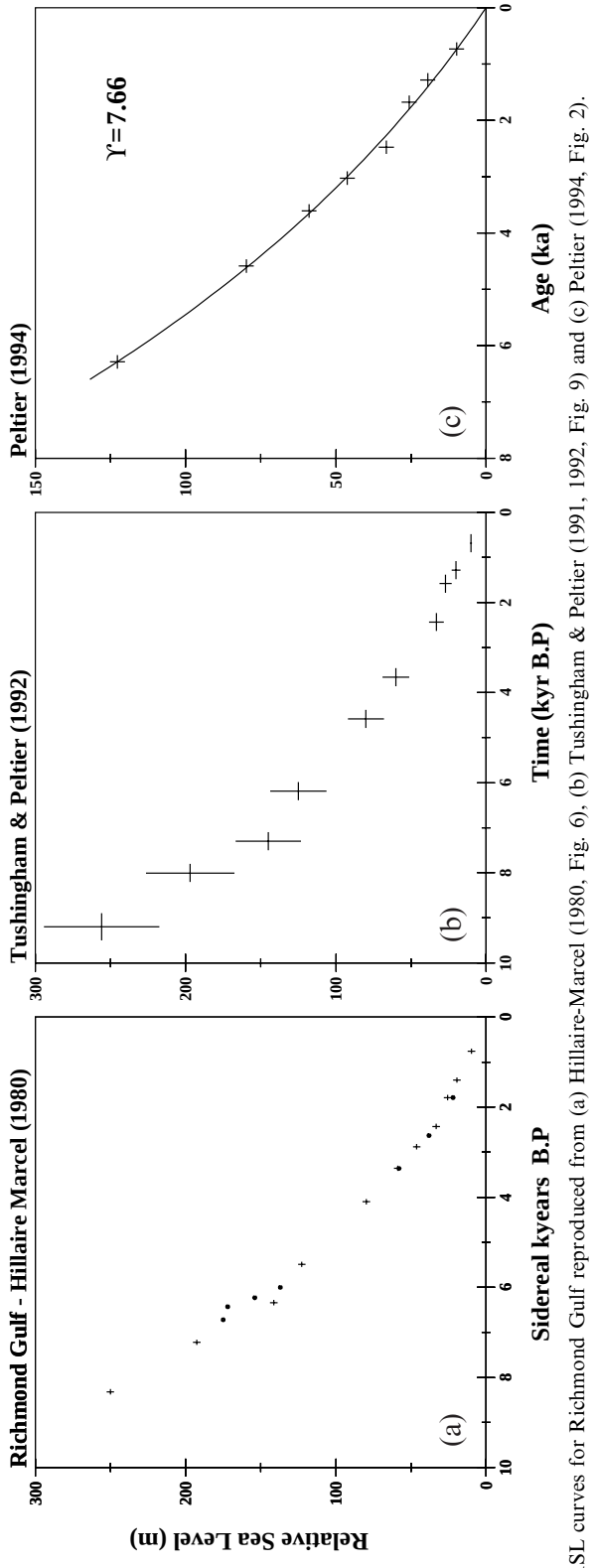

Figure 2. RSL curves for Richmond Gulf reproduced from (a) Hillaire-Marcel (1980, Fig. 6), (b) Tushingham & Peltier (1991, 1992, Fig. 9) and (c) Peltier (1994, Fig. 2).

(age 2.63 kyr) and Richmond Gulf (ages 6.00, 6.23, 6.43 and 6.72 kyr). These ages all refer to C14 dates; however, following Hillaire-Marcel (1980, Fig. 6), we plot these data without correcting the timescale to sidereal ages (despite the label that Hillaire-Marcel adopted for the abscissa).

The Tushingham & Peltier (1991) database of RSL histories includes the Richmond Gulf site and, in this case, adopts 10 of the data points constructed by Hillaire-Marcel (1980) under the assumption of a 45 yr cyclicity in beach formation (that is, the crosses in Fig. 2(a) with the exception of the data point of age $\sim$3 kyr). Our examination of this database has revealed an important error: Tushingham & Peltier (1991) assumed that the ages cited by Hillaire-Marcel (1980) for these 10 data points were C14 ages, rather than sidereal ages. In all likelihood, Tushingham & Peltier (1991) assumed that these data points, like those obtained by survey [Hillaire-Marcel (1980, Fig. 6) and the dots in Fig. 2(a)], were plotted in C14 time.

To confirm this assertion we reproduce RSL constraints for Richmond Gulf shown in Fig. 9 of Tushingham & Peltier (1992) (including the label for the abscissa axis, which is intended to refer to sidereal age) (Fig. 2b). In this case, the dimensions of the cross symbols reflect uncertainties in age and height adopted by Tushingham and Peltier in their 1991 database. One can easily verify that the age–height pairs in Fig. 2(b) can be generated by assuming that the crosses in the left frame of the same figure have C14 ages and then applying the usual C14-to-sidereal correction. The effect of this correction is to reduce the curvature of the RSL curve (since the correction is generally increasingly positive for progressively older data).

The result of this error can be seen in Fig. 2(c). This figure is reproduced from Peltier (1994, Fig. 2). It is unclear whether Peltier (1994) ascribed any significance to the dimensions of the cross symbols. The abscissa axis (also reproduced from Peltier 1994) refers to sidereal time. The RSL data in this figure were derived, like those in the middle frame, from the Hillaire-Marcel (1980) 45 yr cycle data (crosses, left frame) by assuming that the latter ages were in C14 time and unnecessarily performing a C14-to-sidereal mapping. In this regard, Peltier (1994) included the $\sim$3 kyr data point omitted by Tushingham & Peltier (1991, 42) and only used the eight youngest data points in the Hillaire-Marcel (1980) record. The solid line in the figure, also reproduced from Peltier (1994), shows the best-fitting exponential form (2) through the data. The best-fitting decay time for this form is 7.66 kyr, as also determined by Peltier (1994).

More recently, Peltier (1998) argued that the 7.6 kyr decay time cited for Richmond Gulf is suspect because it 'contained very few [uncalibrated] carbon dates' (p. 651). In fact, errors in the past estimate of the decay time, including the original published estimate of Peltier (1994), are due to an error in the Tushingham & Peltier (1991) database entry for Richmond Gulf.

4 SEA-LEVEL TRENDS IN SOUTHEASTERN HUDSON BAY

In Table 1 we provide a recompilation of RSL data from southeastern Hudson Bay. The locations of sites discussed in the table are given in Fig. 1. In most cases, the individual data are clustered in a reasonably small area within the site specified in the table (e.g. within Castle Island, Richmond Gulf, etc.). Exceptions are the James Bay data originally compiled (and in many cases collected) by Hardy (1976). Following Hardy (1976) we use the numbers 1 to 22 to specify these data, and the associated locations are given in the bottom right inset in Fig. 1. In this regard, Table 1 also indicates whether Hardy (1976) used a particular datum in constructing his emergence curve for the region [as an example, GSC-2239 or Hardy (1976, 9N) is data point 9 in his compilation, and he excluded it from his plotted emergence curve].

Our Table 1 is revised in several respects from the recompilation of data from southeastern Hudson Bay by Peltier (1998). First, we add a set of data not included in this recompilation, primarily from the sites Poste de la Baleine, Petite Riviere de la Baleine, Fort George and Cape Henrietta Maria. [We note that the data from Cape Henrietta Maria were included in the classic study by Walcott (1972).] Second, we omit three data points from the site Povungnituk (see Fig. 1) because the site is not located in the southeastern part of the Bay (we return to this point later). We also omit a small number of other data, as discussed in Appendix A. Finally, we correct a number of errors in the Peltier (1998) recompilation, and these corrections are also described in Appendix A.

A majority of the available constraints from the region are derived from a rather small number of sources that date back nearly two decades or more (Hillaire-Marcel 1976; Allard & Tremblay 1983; Hardy 1976). Furthermore, the database is formed by a widely distributed set of sites; indeed, the greatest separation exceeds 500 km.

To illustrate the trends associated with the data, and to facilitate later discussion, we plot site-specific relative sea-level curves in Fig. 3. The boxes and diagonal crosses in the various panels are data included in the Peltier (1998) compilation (corrected, if necessary, as discussed in the Appendix), with the latter denoting constraints excluded by him because they are 'clearly displaced below sea level' (Peltier 1998, p. 612). Although we might concur with some of these exclusions (some of the shell data at Merry Island older than about 3 kyr), other exclusions are more problematic. For example, Peltier (1998) drops the Mytilus edulis sample at time 0.0 at Castle Island (GSC-2470; notice the cross centred on the origin). This exclusion is apparently motivated by the height of the sample (0.0) relative to the young driftwood samples at the same site (which cluster about 10 m above present sea level). However, the youngest Mytilus edulis sample is entirely consistent with the sea-level trend defined by the older Mytilus edulis samples at Castle Island, and one could certainly alternately conclude that the driftwood constraints at Castle Island are anomalous. In fact, this would be more likely since wood floats; indeed, there are other examples in Fig. 3 where young driftwood samples appear to be displaced upwards relative to the prevailing sea-level trend (e.g. the $t=0$ and $t=120$ yr driftwood data at Neilsen Island; the former is not visible in Fig. 3). This issue is clearly important, since the postglacial decay time at Castle Island inferred by excluding the Mytilus edulis sample at $t=0$ would be significantly shorter than the decay time inferred if one were to omit, instead, the driftwood samples.

5 ESTIMATING POSTGLACIAL DECAY TIMES: A REVISED METHODOLOGY

Previously described methods for estimating postglacial decay times have made a number of assumptions whose validity has yet to be explored in detail. For example, it is unclear to what

Table 1. Data From SE Hudson Bay.

Age(C14)	Height (m)*	Lab. No.	Material†	Peltier (1998)§	Reference¶
Richmond Gulf					
4070.0 ± 140.0	24.0	GSC-1326	H	N	Hillaire-Marcel (1976) after Haselton
6000.0 ± 160.0	137.0	GSC-1287	M	Y‡	Hillaire-Marcel (1976) after Haselton
6000.0 ± 210.0	153.0	GSC-1725	H	N	Walcott (1980) after Haselton
6230.0 ± 220.0	154.0	GSC-1364	M	Y	Hillaire-Marcel (1976) after Haselton
6235.0 ± 110.0	110.0	I-8364	S		Hillaire-Marcel (1976)
6390.0 ± 180.0	77.0	GSC-1328	M	N	Hillaire-Marcel (1976) after Haselton
6430.0 ± 150.0	172.0	GSC-1261	M	Y	Hillaire-Marcel (1976) after Haselton
6720.0 ± 150.0	175.0	GSC-1238	H	Y‡	Hillaire-Marcel (1976) after Haselton
Castle Island					
0.0 ± 60.0	0.0	GSC-2470	M	N	Lowdon & Blake (1980)
130.0 ± 100.0	9.1	Qu-1210	D	Y	Allard & Tremblay (1983)
210.0 ± 80.0	9.1	Qu-1201	D	Y	Allard & Tremblay (1983)
890.0 ± 100.0	13.3	Qu-1064	M	Y	Allard & Tremblay (1983)
1790.0 ± 50.0	22.0	GSC-2074	M	Y	Walcott & Craig (1975)
2030.0 ± 60.0	29.0	GSC-2129	M	Y	Walcott (1980)/Lowdon & Blake (1980)
2760.0 ± 80.0	44.0	GSC-2348	M	Y	Walcott (1980)/Lowdon & Blake (1980)
3360.0 ± 60.0	58.0	GSC-2070	M	Y	Walcott & Craig (1975)
3460.0 ± 90.0	16.0	Qu-1065	S	N	Allard & Tremblay (1983)
Poste de la Baleine/Great Whale River					
3150.0 ± 50.0	27.0	L-441A	D		Lee (1960)
3300.0 ± 110.0	62.0	GIF-1567	C	N‡	Plumet (1974)
4580.0 ± 80.0	90.0	GSC-2432	P		Lowdon & Blake (1980)
4780.0 ± 110.0	110.0	GSC-2354	P		Lowdon & Blake (1980)
7310.0 ± 260.0	120.0	GSC-1543	P		Lowdon & Blake (1980)
Petite Riviere de la Baleine					
2630.0 ± 85.0	38.0	I-8367	P		Hillaire-Marcel (1976)
4740.0 ± 110.0	47.0	CSC-27	D		Hillaire-Marcel (1976)
6380.0 ± 110.0	0.0	I-8362	A		Hillaire-Marcel (1976)
6420.0 ± 240.0	94.0	GSC-595	H		Lowdon *et al.* (1967)
7820.0 ± 100.0	0.0	Qu-280			Hillaire-Marcel (1976)
Neilsen Island					
0.0 ± 0.0	5.0	Qu-1211	D	N	Allard & Tremblay (1983)
120.0 ± 90.0	7.6	Qu-1108	D	Y	Allard & Tremblay (1983)
490.0 ± 80.0	8.9	Qu-1068	M	Y	Allard & Tremblay (1983)
580.0 ± 70.0	13.2	Qu-1081	M	Y	Allard & Tremblay (1983)
720.0 ± 80.0	8.5	Qu-1107	D	Y	Allard & Tremblay (1983)
1490.0 ± 90.0	17.3	Qu-1106	M	Y	Allard & Tremblay (1983)
1680.0 ± 90.0	18.8	Qu-1105	M	Y	Allard & Tremblay (1983)
1760.0 ± 90.0	20.4	Qu-1104	M	Y	Allard & Tremblay (1983)
2020.0 ± 100.0	23.7	Qu-1102	M	Y	Allard & Tremblay (1983)
2026.0 ± 100.0	27.3	Qu-1100	M	Y	Allard & Tremblay (1983)
2050.0 ± 100.0	21.9	Qu-1103	M	Y	Allard & Tremblay (1983)
2230.0 ± 100.0	29.9	Qu-1098	M	Y	Allard & Tremblay (1983)
2260.0 ± 100.0	26.6	Qu-1101	M	Y	Allard & Tremblay (1983)
2430.0 ± 100.0	28.9	Qu-1099	M	Y	Allard & Tremblay (1983)
2470.0 ± 100.0	31.7	Qu-1097	M	Y	Allard & Tremblay (1983)
Manitounuk Peninsula					
330.0 ± 100.0	13.5	Qu-1293	D		Allard & Tremblay (1983)
480.0 ± 90.0	4.7	Qu-1299	D	N	Allard & Tremblay (1983)
670.0 ± 80.0	4.7	Qu-1298	M	Y	Allard & Tremblay (1983)
770.0 ± 110.0	54.7	Qu-1289	P		Allard & Tremblay (1983)
1590.0 ± 90.0	1.5	Qu-1291	D		Allard & Tremblay (1983)

Table 1. (*Continued.*)

Age(C14)	Height (m)*	Lab. No.	Material†	Peltier (1998)§	Reference¶
1680.0 ± 90.0	8.0	Qu-1292	S	N	Allard & Tremblay (1983)
1830.0 ± 240.0	50.0	Qu-1297	L		Allard & Tremblay (1983)
2410.0 ± 90.0	31.5	Qu-1295	M	Y	Allard & Tremblay (1983)
2510.0 ± 80.0	32.0	Qu-1296	M	Y‡	Allard & Tremblay (1983)
2860.0 ± 100.0	34.3	Qu-1288	M	Y	Allard & Tremblay (1983)
3480.0 ± 100.0	52.3	Qu-1290	M	Y	Allard & Tremblay (1983)
4270.0 ± 100.0	65.0	Qu-1294	S	Y	Allard & Tremblay (1983)
Merry Island					
150.0 ± 80.0	5.5	Qu-1206	D	Y	Allard & Tremblay (1983)
160.0 ± 100.0	4.8	Qu-1209	D	Y‡	Allard & Tremblay (1983)
180.0 ± 80.0	6.8	Qu-1208	D	Y	Allard & Tremblay (1983)
350.0 ± 80.0	6.3	Qu-1205	D	Y	Allard & Tremblay (1983)
400.0 ± 90.0	8.9	Qu-1207	D	Y	Allard & Tremblay (1983)
570.0 ± 90.0	12.9	Qu-1204	D	Y	Allard & Tremblay (1983)
680.0 ± 80.0	12.9	Qu-1203	D	Y	Allard & Tremblay (1983)
720.0 ± 80.0	12.9	Qu-1202	D	Y	Allard & Tremblay (1983)
1360.0 ± 230.0	15.2	Qu-1084	S	Y	Allard & Tremblay (1983)
1680.0 ± 390.0	21.4	Qu-1087	M	Y‡	Allard & Tremblay (1983)
2560.0 ± 350.0	10.4	Qu-1085	S	N	Allard & Tremblay (1983)
2720.0 ± 370.0	6.3	Qu-1086	S	N	Allard & Tremblay (1983)
2780.0 ± 110.0	15.2	Qu-1083	S	N	Allard & Tremblay (1983)
3160.0 ± 360.0	19.2	Qu-1082	S	N	Allard & Tremblay (1983)
3310.0 ± 100.0	6.4	Qu-1066	S	N	Allard & Tremblay (1983)
4420.0 ± 100.0	6.4	Qu-1067	S	N‡	Allard & Tremblay (1983)
Bill of Portland‡					
0.0 ± 0.0	11.8	Qu-1089	D	N	Allard & Tremblay (1983)
0.0 ± 0.0	7.0	Qu-1091	D	N‡	Allard & Tremblay (1983)
20.0 ± 80.0	4.5	Qu-1096	D	Y	Allard & Tremblay (1983)
40.0 ± 80.0	6.2	Qu-1092	D	Y	Allard & Tremblay (1983)
60.0 ± 80.0	4.5	Qu-1095	D	Y	Allard & Tremblay (1983)
70.0 ± 90.0	5.6	Qu-1094	D	Y	Allard & Tremblay (1983)
130.0 ± 80.0	7.0	Qu-1090	D	Y	Allard & Tremblay (1983)
150.0 ± 100.0	10.3	Qu-1212	D	Y	Allard & Tremblay (1983)
190.0 ± 90.0	6.2	Qu-1093	D	Y	Allard & Tremblay (1983)
410.0 ± 80.0	11.8	Qu-1088	D	Y	Allard & Tremblay (1983)
James Bay—Fort George					
3700.0 ± 130.0	53.3-57.9	L-433A	D	Y‡	Farrand (1962)
2685.0 ± 90.0	10.0	I-7993	O		Hillaire-Marcel (1976) after Dionne
1780.0 ± 90.0	15.0	I-7994	O		Hillaire-Marcel (1976) after Dionne
1500.0 ± 85.0	10.0	I-7995	O		Hillaire-Marcel (1976) after Dionne
James Bay—Hardy (1976)					
4470.0 ± 170.0	16.0 ± 1	Qu-248	S	N	Hardy (1976; 1N)
4110.0 ± 120.0	40.0 ± 1	Qu-121	S	N	Hardy (1976; 2Y)
5080.0 ± 180.0	100.0 ± 1	Qu-256	H	Y‡	Hardy (1976; 3Y)
5560.0 ± 130.0	125.0 ± 1	Qu-119	S	Y	Hardy (1976; 4Y)
6810.0 ± 200.0	180.0 ± 1	Qu-255	S	Y‡	Hardy (1976; 5Y)
6910.0 ± 350.0	186.0 ± 1	Qu-247	S	Y	Hardy (1976; 6Y)
7110.0 ± 180.0	183.0 ± 1	Qu-245	S	Y	Hardy (1976; 7Y)
6810.0 ± 80.0	168.0 ± 1	GSC-2244	H	Y	Hardy (1976; 8N)
7290.0 ± 90.0	175.0 ± 1	GSC-2239	S	N	Hardy (1976; 9N)
6500.0 ± 90.0	174.0 ± 1	GSC-1959	S	Y	Hardy (1976; 10Y) after Vincent
6660.0 ± 190.0	177.0 ± 1	Qu-249	S	Y	Hardy (1976; 11Y)
7880.0 ± 160.0	289.0 ± 1	Qu-122	S	N‡	Hardy (1976; 12Y)
7750.0 ± 180.0	287.0 ± 1	Qu-124	S	N‡	Hardy (1976; 13Y)

Table 1. (*Continued.*)

Age(C14)	Height (m)*	Lab. No.	Material†	Peltier (1998)§	Reference¶
7370.0 ± 100.0	245.0 ± 1	Qu-369	S	Y	Hardy (1976; 14Y)
6930.0 ± 190.0	195.0 ± 4	Qu-250	S	Y	Hardy (1976; 15Y)
6950.0 ± 210.0	201.0 ± 1	Qu-253	S	Y	Hardy (1976; 16Y)
7440.0 ± 210.0	215.0 ± 3	Qu-258	S	Y	Hardy (1976; 17Y)
7440.0 ± 180.0	15.0 ± 1	Qu-368	S	N	Hardy (1976; 18N)
7140.0 ± 210.0	225.0 ± 1	Qu-254	S	Y	Hardy (1976; 19Y)
7030.0 ± 210.0	231.0 ± 1	Qu-252	S	Y‡	Hardy (1976; 20Y)
7110.0 ± 110.0	203.0 ± 1	GSC-2161	S	Y‡	Hardy (1976; 21N) after Vincent
7120.0 ± 210.0	203.0 ± 1	Qu-370	S	Y	Hardy (1976; 22N)
7360.0 ± 100.0	203.0 ± 1	GSC-2135	S	Y	Hardy (1976; 22bN) after Vincent
Cape Henrietta Maria					
235.0 ± 190.0	7.4	I-3908	D		Webber *et al.* (1970)
1430.0 ± 190.0	22.6	I-3983	M		Webber *et al.* (1970)
2310.0 ± 200.0	40.6	I-3909	M		Webber *et al.* (1970)
7400.0 ± 140.0	137.7	GSC-877	S		Craig (1969)
5600.0 ± 200.0	128.2	GSC-245			Walcott (1972)
7250.0 ± 160.0	122.5	GSC-872			Walcott (1972)

*In our analysis of these data we adopt the rule for height errors specified by Peltier (1998). These errors are assumed to be 5 per cent of the height, with minimum and maximum values of 0.5 m and 2.5 m, respectively. Exceptions are specified in the table.
†Material samples are denoted as follows. M: Mytilus edulis; S: shells or mixed shells; H: Hiatella arctica; D: driftwood or wood; P: peat; O: organic material; A: Portlandia arctica; L: lacustrine sediments; C: charcoal.
§This column is blank if the datum does not appear in the recent Peltier (1998, Table 1) literature review. Otherwise, Y (yes) and N (no) denote whether Peltier (1998) adopted the data in his analysis of postglacial sea level.
¶References in which the associated datum is discussed. In the case of Hardy (1976) our citation specifies the locality listed by Hardy (1976) (1–22) and shown in our Fig. 1, as well as whether the datum was used by Hardy (1976) to construct his 'emergence curve' (Y/N). All height entries reflect corrections applied by Hardy.
‡Denotes revision/corrections to the Peltier (1998) database.

extent decay times are contaminated from global changes in ocean volume associated with ongoing melting of Late Pleistocene ice sheets (e.g. Mitrovica & Forte 1997). A second assumption involves the practice of lumping together data from different geographic regions and inferring decay times on the basis of the composite RSL trends. We explore these issues using numerical simulations of RSL histories in southeastern Hudson Bay. Our synthetic RSL data are computed using a spherically symmetric, self-gravitating, Maxwell viscoelastic earth model. The elastic structure of the model is given by PREM (Dziewonski & Anderson 1981). Furthermore, the model is defined by a 120-km-thick elastic lithosphere and upper and lower mantle viscosities of 10^{21} and 3×10^{21} Pa s, respectively (we place no particular emphasis on this model and use it simply as an example). The ice model adopted in the calculation is adapted from the ICE-3G deglaciation model of Tushingham & Peltier (1991) in order to add a glaciation phase and prior glacial cycles. We compute gravitationally self-consistent sea-level variations on the earth model including both perturbations to the rotation vector and time-dependent evolution of continental margins (Milne *et al.* 1999).

A prediction of the RSL history at Richmond Gulf for integer ages back to 12 kyr BP is shown by the lower set of solid dots in Fig. 4(a). We have performed a simple Monte Carlo search for the 'best-fitting' form (3) through a subset of the predicted RSL 'data' with ages less than 9 kyr (i.e. RSL(t), for $t = 0, 1, 2, \ldots 8$ kyr BP). The search explored the space (A, τ, c). The dashed line in Fig. 4(a) is the best-fitting form (71 m, 6.58 kyr, 0.0 m) determined from this exercise. In addition, the dashed line in Fig. 5 shows the misfit as a function of the decay time adopted in the Monte Carlo search. The misfit is defined as

$$M = \frac{\sqrt{\sum_{n=1}^{N} \{\mathrm{RSL}_{\mathrm{model}}(t_n) - \mathrm{RSL}_{\mathrm{data}}(t_n)\}^2}}{N}, \qquad (4)$$

where N is the total number of data points ($N = 9$) and $\mathrm{RSL}_{\mathrm{model}}$ and $\mathrm{RSL}_{\mathrm{data}}$ represent predictions based on the form (3) and the full viscoelastic calculation, respectively.

The minimum for the misfit is rather sharply peaked at a value of 6.58 kyr (Fig. 5). Furthermore, the absolute value of the misfit (0.1) is small, indicating that the form (3) is a very accurate model for the predicted postglacial RSL variation at Richmond Gulf, at least over the time window extending to 8 kyr BP. This performance is evident in Fig. 4(a), where the dashed line clearly passes accurately through the numerical RSL predictions based on the viscoelastic response calculations.

Next we explore the bias introduced into the decay time estimate by meltwater entering the global oceans during the period sampled by our 8 kyr time window. The upper trend of solid dots in Fig. 4(a) was derived by correcting the results based on the full sea-level theory (the lower trend of solid dots) by the eustatic sea-level curve associated with our adopted ice model (ICE-3G). Subtracting out the 'meltwater' signal clearly increases the amplitude of the monotonic sea-level fall at Richmond Gulf. Note that the discrepancy between the two trends ceases at 5 kyr BP, which represents the time of cessation of deglaciation in the ICE-3G model.

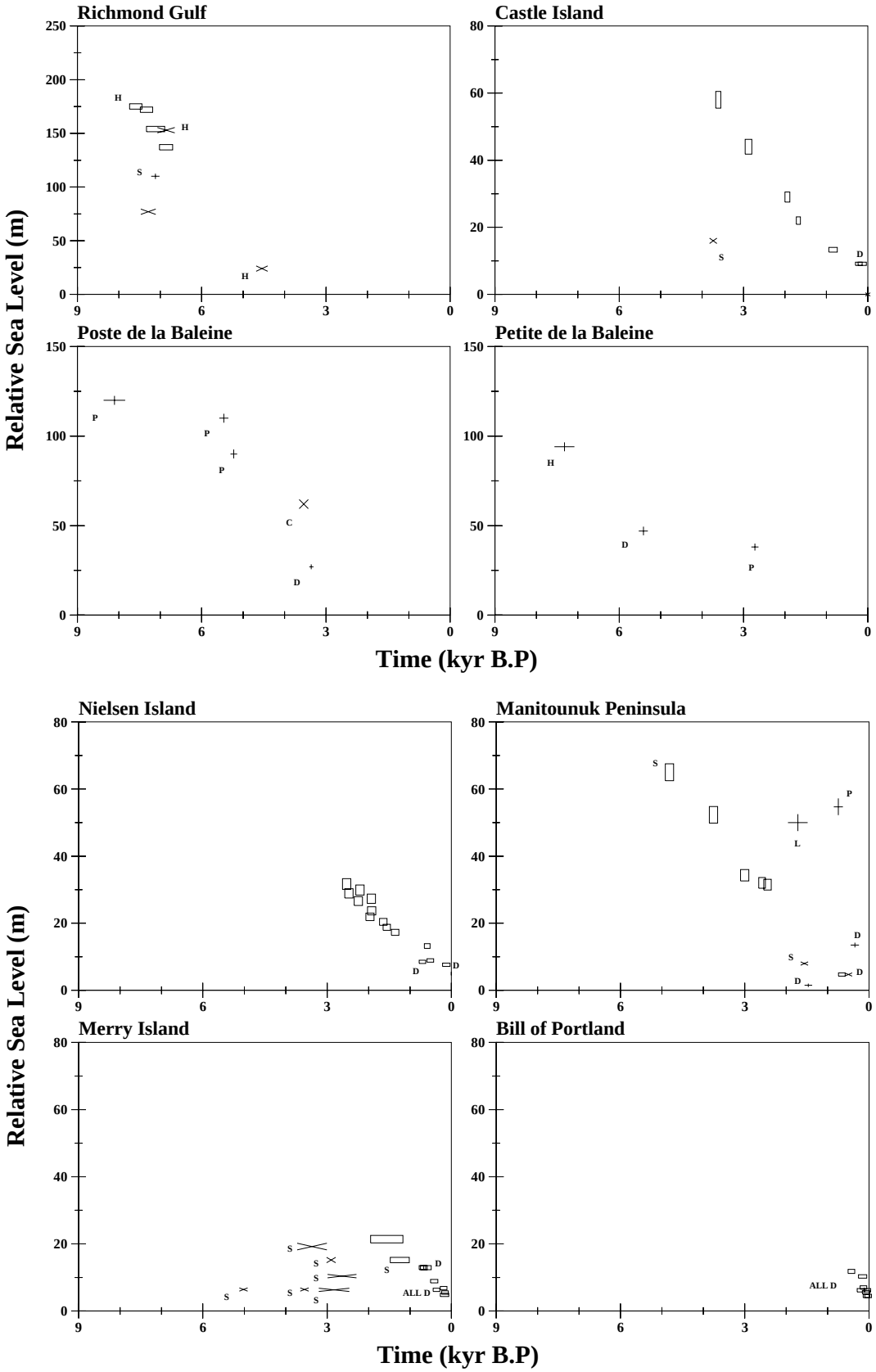

Figure 3. Plots of the RSL observations in southeastern Hudson Bay compiled in Table 1. The boxes represent data included in the compilation of Peltier (1998) that are used in his analysis of a postglacial decay time for the region. The diagonal crosses are data that appear in the same compilation but are excluded from his analysis of the postglacial decay time. Vertical–horizontal crosses are data not appearing in the Peltier (1998) compilation. Letters on the plots denote material associated with the datum. As in Table 1, these are S: shells or mixed shells; H: Hiatella arctica; D: driftwood or wood; P: peat; O: organic material; A: Portlandia arctica. Data without a label denote Mytilus edulis samples (M in Table 1).

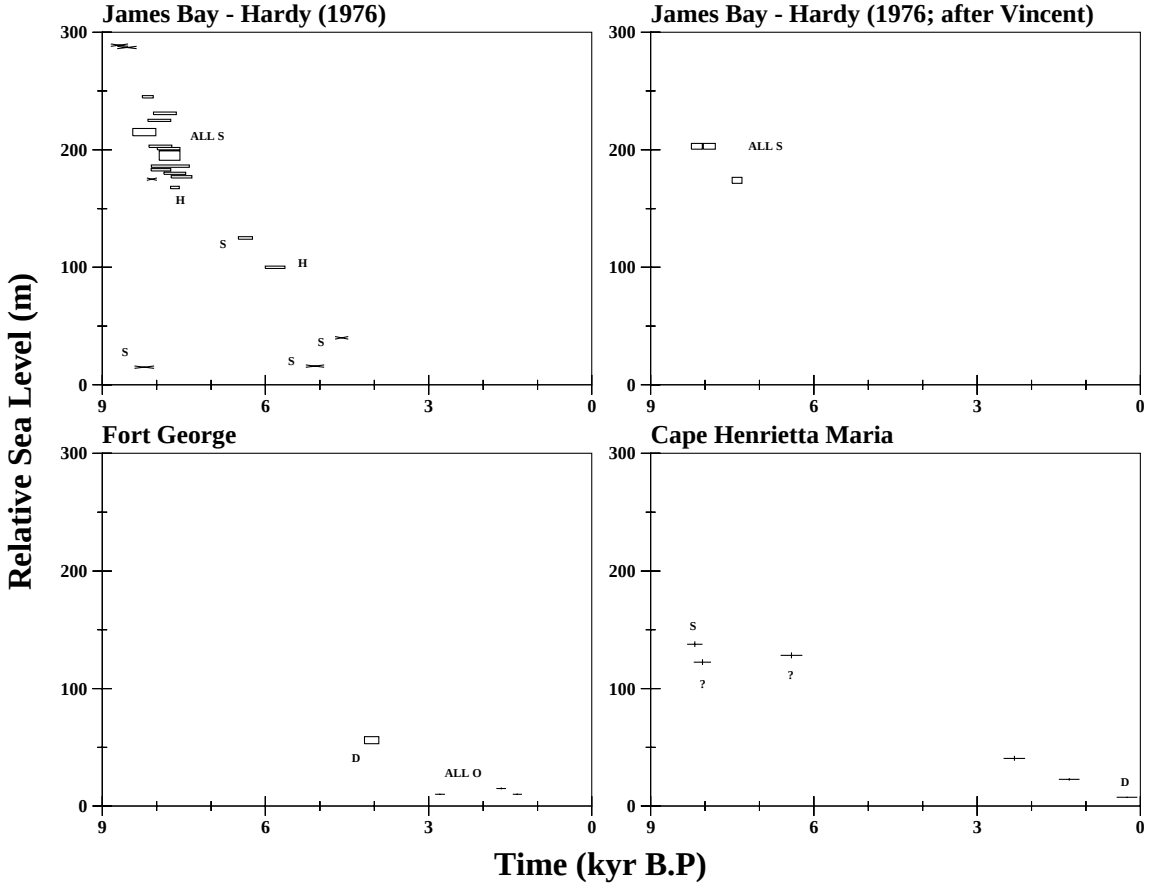

Figure 3. (*Continued.*)

The dotted lines in Figs 4(a) and 5 are analogous to the dashed lines in the same figures, with the exception that they represent Monte Carlo results for this 'corrected' sea-level history. The observational record from southeastern Hudson Bay extends to roughly 8–9 kyr BP (Fig. 3). The results in Figs 4 and 5 indicate that estimates of postglacial decay times using a time window of this extent may be biased on the order of 1 kyr too high by neglecting the influence of eustatic changes

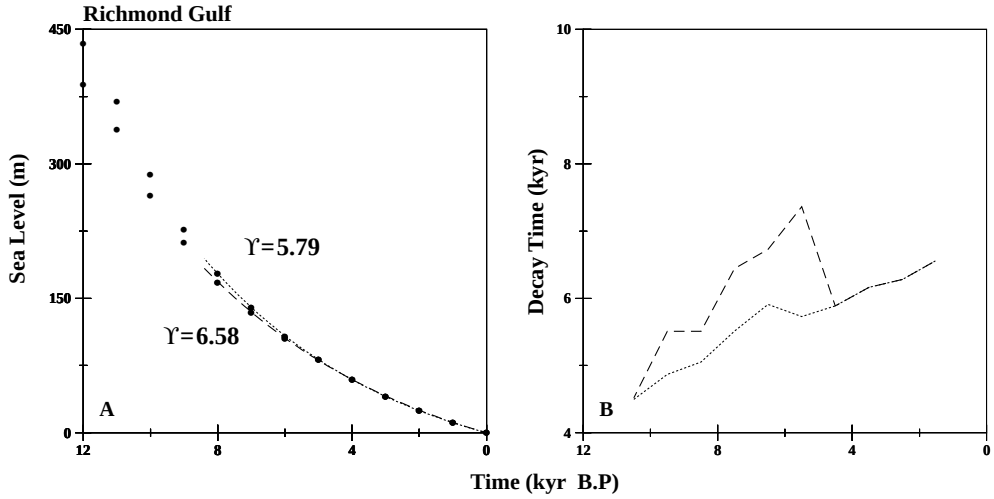

Figure 4. Decay time analysis of a synthetic set of RSL 'data' at Richmond Gulf computed using the ice history and viscoelastic earth model discussed in the text. (a) The lower set of dots represents the synthetic RSL data, while the upper set is corrected from the lower by subtracting out the eustatic sea-level variation associated with the adopted ice model. The dashed and dotted lines represent the best-fitting exponential form (3) through each set of data. In this exercise we use only 'data' with ages less than 9 kyr. The decay times associated with the best fit are given by the labels. (b) Evolution of the best-fitting decay time over the last $\sim$10 kyr for the synthetic RSL data (dashed line) and the version of these data corrected for eustatic sea-level trends (dotted line). These decay times are determined using a subset of three RSL points, one being the origin ($t=0$) and the other two being successive points on the RSL curves ($t=10$ and 11, 9 and 10, 8 and 9, etc.)

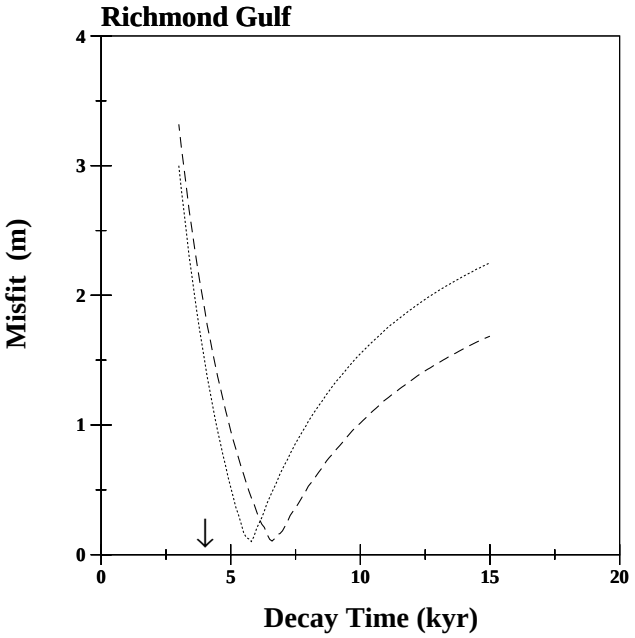

Figure 5. Misfit of the best-fitting form (3) as a function of decay time for the synthetic RSL data shown in Fig. 4(a). The Monte Carlo procedure is only applied to data with ages less than 9 kyr. The dashed and dotted lines refer to misfit curves for the lower and upper sets of solid dots in Fig. 4(a) (the latter are corrected for the influence of eustatic sea-level trends). The arrow denotes the global best-fitting decay time determined from a composite RSL history constructed by combining predictions for Richmond Gulf and James Bay shown in Fig. 6 (see text).

in global sea level. Our analysis of the observational record in subsequent sections of this paper will therefore include a correction for these eustatic sea-level changes.

The response of a radially stratified viscoelastic earth model to an applied surface mass load is characterized, at each spherical harmonic degree, by a multiplicity of modes of pure exponential decay (Peltier 1976). Although our single-exponential form (3) is an accurate model for postglacial sea-level trends (left frame of Fig. 4), the decay time associated with this form must, nevertheless, be understood as a measure of the response that is 'lumped' over both time and space (i.e. spherical harmonic degree). To examine the temporal evolution of the decay time, we have computed the best-fitting decay time for a subset of the numerically predicted RSL 'data' (dots in Fig. 4) comprising three points: RSL(t_n), RSL(t_{n-1}) and RSL($t=0$) (that is, two adjacent points on the sea-level curve and the origin). The procedure is repeated for a suite of n values, and the results are shown in Fig. 4(b) [the decay time determined for each triplet is plotted against a value of $t=(t_n+t_{n-1})/2$].

The contamination of the RSL signal, and hence the decay time, by eustatic sea-level changes prior to 5 kyr BP is evident in Fig. 4(b). The decay times determined for the 8 kyr sea-level curves in Fig. 4(a) (5.79 or 6.58 kyr) are clearly averages associated with a time-dependent decay constant, with decay times varying by several kiloyears from 10 kyr BP to the present in Fig. 4(b). The natural decay time increases with time, reflecting the fact that the shorter decay times associated with the multi-exponential response relax from the system quickest. This evolution in the decay time is cautionary in the sense that forward predictions of observationally inferred decay times must adopt a time window consistent with these observations. Furthermore, variations in decay times inferred from geological data may result, in part, from differences in the time window sampled by the data.

In Fig. 6 we plot synthetic RSL variations, predicted using the same 'test' ice and earth models described above, for various sites in southeastern Hudson Bay. The label 'JB' refers to two predictions: one for a site at the southern portion of the James Bay inset in Fig. 1 and the other for a site within the northern part of this inset (the former is of higher amplitude than the latter). The label 'RG' refers to a set of predictions: one for Richmond Gulf and the rest for sites in the southern part of the top inset in Fig. 1. These latter sites have RSL trends that are almost indistinguishable from one another and that are of slightly higher amplitude than the prediction for the Richmond Gulf site. Finally 'PV' represents the prediction for Povungnituk (see Fig. 1).

The RSL trend at Povungnituk is clearly distinct from predictions in the Richmond Gulf and James Bay regions. Accordingly, in contrast to the Peltier (1998) recompilation for southeastern Hudson Bay, we have chosen not to incorporate observational constraints from this area into our own recompilation.

The best-fitting decay times determined from the numerically predicted trends 'RG' and 'JB' over the last 8 kyr in Fig. 6 are all near 5.8 kyr (in the case when these curves are corrected for eustatic sea-level trends, as in Fig. 4). Thus, for the spherically

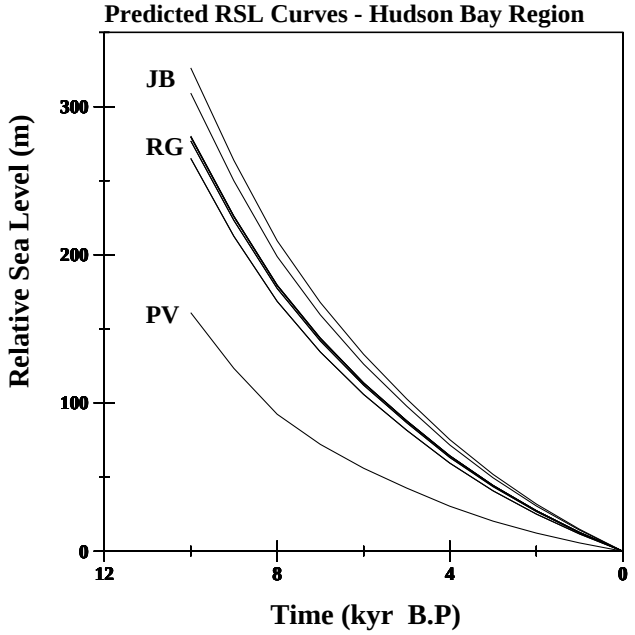

Figure 6. Synthetic RSL curves predicted using the ice history and viscoelastic earth model described in the text. The curve labelled PV refers to the site Povungnituk (Fig. 1). The two curves labelled JB refer to sites in the northern (53.5°N) and southern (52°N) parts of the James Bay inset in Fig. 1. The former has the smaller amplitude. The set of curves labelled RG are for sites within the Richmond Gulf inset of Fig. 1. The thick cluster of overlapping curves includes results for Castle Island, Neilsen Is., Poste de la Baleine, Petite Riviere de la Baleine, Merry Island, Bill of Portland and Manitounuk Peninsula. The single curve slightly below this cluster was obtained for the Richmond Gulf site.

symmetric earth model adopted here, the decay time that characterizes each site does not vary significantly over the region sampled in the insets to Fig. 1. Nevertheless, the amplitudes of the 'JB' and 'RG' sea-level trends in Fig. 5 differ by about 20 per cent, and therefore computing a single decay time from a composite RSL curve constructed from constraints taken from both regions may be suspect. The nature of the geological constraints shown in Fig. 3 is less than optimal in this regard. C14 data from sites within the northern inset (including Richmond Gulf, Castle Island, Merry Island, Neilsen Island, Manitounuk Peninsula, etc.) are primarily younger than about 5 kyr. In contrast, observational constraints from the James Bay inset are strongly biased towards ages greater than 5 kyr (see Fig. 3). We will see in the next section that this situation is aggravated further when a subset of 'consistent' sea-level constraints is established for the region.

To explore this bias, we derive a composite synthetic sea-level data set by combining our numerical viscoelastic predictions for the sites in southern James Bay (for ages older than 6 kyr BP) and Richmond Gulf (ages younger than 6 kyr). We determine a 'best-fitting' decay time for this composite synthetic record (corrected for eustatic trends) using the Monte Carlo procedure described above. This best-fitting decay time is shown by the location of the vertical arrow in Fig. 5. The value of the decay time, 4.1 kyr, is $\sim$2 kyr shorter than the decay time determined from data at either Richmond Gulf or James Bay (5.8 kyr). This bias results from combining the young, relatively low-amplitude Richmond Gulf data and the old, relatively high-amplitude James Bay data, thus producing a composite sea-level record with significantly more 'curvature' than the individual records (Fig. 6). Peltier (1998) derived a best-fitting decay time for southeastern Hudson Bay (3.426 kyr) by constructing a composite sea-level record using data from James Bay and Richmond Gulf. This combination of data is inappropriate. Our analysis of the observational record appearing in subsequent sections is based on a far more restrictive use of composite records.

Estimation of the decay time for an observationally inferred postglacial sea-level trend must account for errors in both time and space (see Fig. 3). Previous analyses have generally applied eq. (4) (or some minor variation of it) as their measure of fit, with the difference between the observed data and model prediction being normalized by the uncertainty in the height of the datum. Unfortunately, this traditional scheme does not allow for the incorporation of errors in time, which are often the most significant sources of uncertainty in postglacial RSL curves. Accordingly, we adopt a measure of misfit that incorporates errors in both the height and the time dimension (Fig. 7). Consider a model RSL curve generated by applying the triplet (A, τ, c) to the form (3). Such a curve is shown by the solid concave line in Fig. 7. Also consider a single datum, d_n, with height and age errors of Δy and Δt, respectively. Following eq. (4), a traditional measure of the square of the misfit relative to this single datum is

$$M(d_n) = \left(\frac{L'_y}{\Delta y}\right)^2 . \tag{5}$$

Our revised methodology measures misfit, instead, as the smallest 'distance' between the datum and the model curve, where 'distance' in the horizontal direction is measured in dimensionless units $L_t/\Delta t$ and distance in the vertical direction is measured in dimensionless units $L_y/\Delta y$. In practice, this

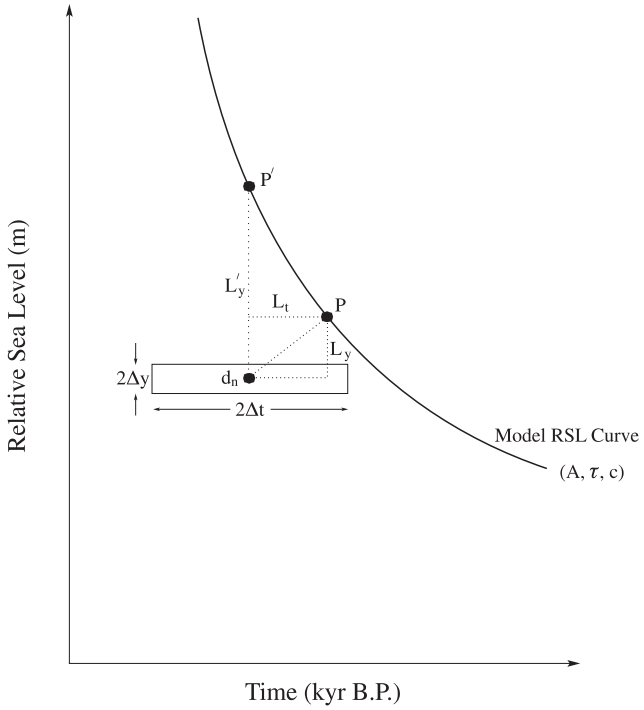

Figure 7. Schematic illustrating the measure of misfit we have adopted in estimating postglacial decay times from the observational record in southeastern Hudson Bay.

smallest distance is computed numerically by simply moving along the model RSL curve (from P' to P and onwards) until we find that $M(d_n)$ is minimized, where eq. (5) is replaced by

$$M(d_n) = \left(\frac{L_y}{\Delta y}\right)^2 + \left(\frac{L_t}{\Delta t}\right)^2 . \tag{6}$$

We denote the numerically determined minimum value as $M_n^{\min}$. The total misfit for the entire RSL curve is then given by

$$M = \frac{\sqrt{\sum_{n=1}^{N} M_n^{\min}}}{N} . \tag{7}$$

The benefits of the new methodology are illustrated in the example shown in Fig. 7. The misfit measured by eq. (5) would be large since $L'_y/\Delta y$ is clearly large. In contrast, inspection of the geometry of Fig. 7 suggests that $M_n^{\min}$ would be of $O(1)$ since it appropriately incorporates the dominance of the age error Δt relative to Δy in this specific case. In our analysis of the observational record for southeastern Hudson Bay we use eqs (6)–(7) to define our misfit within the context of a Monte Carlo search through the space (A, τ, c).

6 NEW ESTIMATES OF POSTGLACIAL DECAY TIMES IN SOUTHEASTERN HUDSON BAY

The synthetic calculations described above serve as a guide for the estimation of decay times in southeastern Hudson Bay. While we consider composite sea-level records, this procedure is constrained so that the sites involved in constructing such a record all fall in only one of the geographic regions defined by the insets in Fig. 1 (that is, no composite will be generated using

samples from both the James Bay and Richmond Gulf regions). Furthermore, since our RSL curves include samples with ages up to ~ 9 kyr, our Monte Carlo search is based on data corrected for geologically inferred eustatic sea-level variations.

The uplift curve for Richmond Gulf generated by Hillaire-Marcel (1980) and based on dated samples is shown by the dots in Fig. 2(a). We have already discussed this curve extensively (we remind the reader that for this data the abscissa axis on the figure should, in fact, refer to C14 time). With reference to Table 1, Hillaire-Marcel (1980) used data collected at Richmond Gulf (GSC-1287, GSC-1364, GSC-1261, GSC-1238), Castle Island (GSC-2070, GSC-2074) and Petite Riviere de la Baleine (I-8367) to construct his 'Richmond Gulf' curve. This curve combines data with a variety of sample types: peat (I-8367), Hiatella arctica (GSC-1238) and Mytilus edulis (the remaining five samples; see Table 1).

In contrast to Hillaire-Marcel (1980), Walcott (1980) advocated using a consistent set of samples in constructing an uplift curve for Richmond Gulf. In particular, he derived 'an uplift curve based solely on the specimens of the shell Mytilus edulis', which he regarded as 'the most representative curve of central regions of uplift' (Walcott 1980, p. 7). The uplift curve included the five Mytilus edulis samples used by Hillaire-Marcel (1980), as well as two additional samples from Castle Island (GSC-2348, GSC-2129). Walcott's (1980) criteria for consistency also extended to the environment of the sample. His data was 'collected from raised beaches of very similar form (all Castle Island samples are from cobble beaches; Walcott & Craig 1975)' (Walcott 1980, p. 7). Walcott's (1980) carefully constructed uplift curve serves as the starting point for our analysis, and it is reproduced by the boxes in Fig. 8(a). [Walcott (1980) listed both raw and 'corrected' elevations; we adopt the former, although the data in Fig. 8(a) include our correction for eustatic sea-level changes, as described above.]

In Fig. 9(a) we show results from our decay time analysis of Walcott's (1980) uplift curve for Richmond Gulf. The plot shows the minimum misfit (computed according to eqs 6 and 7) as a function of the decay time for a set of different choices of the constant shift parameter c (solid lines), as well as the minimum misfit when c is varied from -10 to 10 m (dashed line). The latter curve is relatively flat for decay times greater than about 4–5 kyr, and it increases sharply towards lower decay times. The flatness of the dashed line at long decay times supports Walcott's (1980) argument that a '5000 year minimum [for the decay time] is all that can be claimed by the rebound data' (p. 8).

There is a trade-off between the adopted value of c and the best-fitting decay time determined from the Monte Carlo search (Fig. 9). This is evident in Fig. 8(a), where we plot the best-fitting forms for the cases of $\tau = 4.5$ kyr (dashed line) and 7.5 kyr (dotted line). (The misfit for both cases is ~ 0.38). Simply put, fitting the data with a longer (or shorter) decay time requires that the model RSL curve pass below (or above) the origin. As a result, a value of $c = 6$ m yields the minimum bound of 4.5 kyr for the decay time; in contrast, the best-fit decay time when $c = -3.5$ m is 7.5 kyr (Figs 8a and 9a).

In Fig. 8(b) we extend Walcott's (1980) approach and construct a new RSL curve for the Richmond Gulf region by including all data associated with Mytilus edulis samples within the Richmond Gulf inset of Fig. 1 (with the exception of sample GSC-1328 from Table 1, which is clearly an outlier). The associated misfit analysis is summarized in Fig. 9(b). A comparison of Figs 8(a) and (b) indicates that the new data have ages that are largely clustered within the last 3 kyr. These data have the effect of tightening the bounds on the parameter c. Fig. 9(b) indicates that the minimum misfit as a function of decay time (dashed line) is roughly mapped out by the $c = 0$ m curve, although slightly higher values (up to $c = 3$ m)

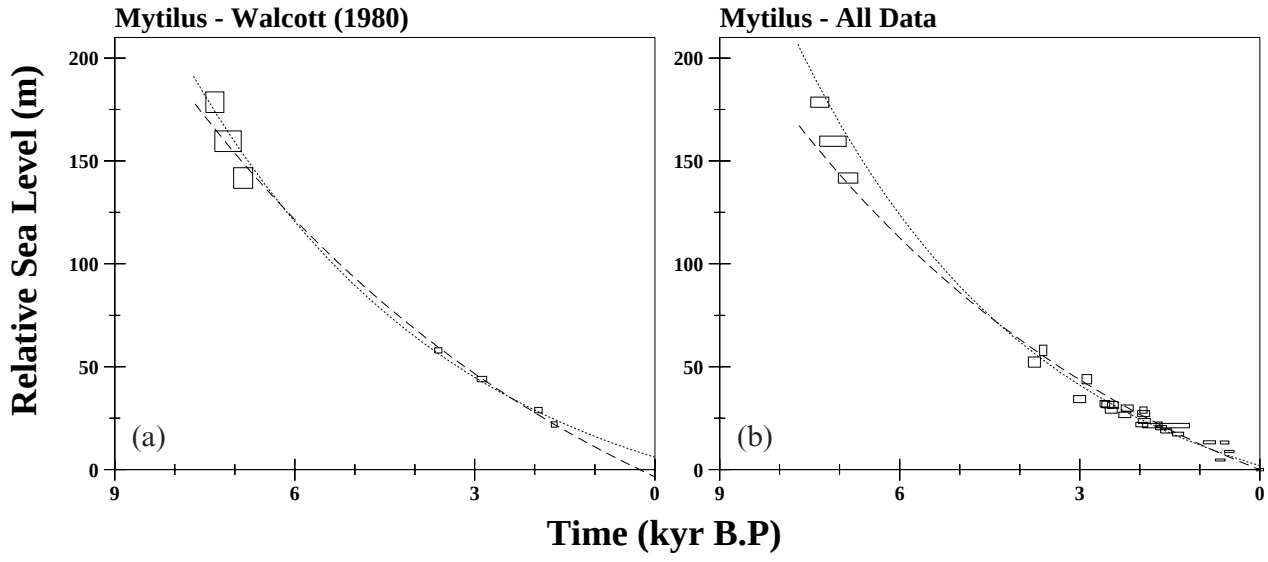

Figure 8. (a) Collection of RSL data adopted by Walcott (1980) to establish an emergence curve for Richmond Gulf and estimate a decay time for the region. The data include the samples GSC-1261, GSC-1364, GSC-1287, GSC-2070, GSC-2348, GSC-2129 and GSC-2074 listed in Table 1. The height errors appearing in the figure are taken directly from Walcott (1980). These samples were chosen by Walcott (1980) to establish a curve based solely on specimens of the shell Mytilus edulis. The dashed and dotted lines represent curves of the form (3) with parameters ($A = 102$ m, $\tau = 7.5$ kyr, and $c = -3.5$ m) and ($A = 41$ m, $\tau = 4.5$ kyr and $c = 6.0$ m), respectively. (b) Collection of all RSL data in Table 1 from sites within the Richmond Gulf inset of Fig. 1 that refer to specimens of the shell Mytilus edulis (with the exception of GSC-1328). In this case we have adopted the rule for height errors described in the table. The dashed and dotted lines represent curves of the form (3) with parameters ($A = 76$ m, $\tau = 6.6$ kyr and $c = 0.0$ m) and ($A = 35$ m, $\tau = 4.0$ kyr and $c = 2.0$ m), respectively.

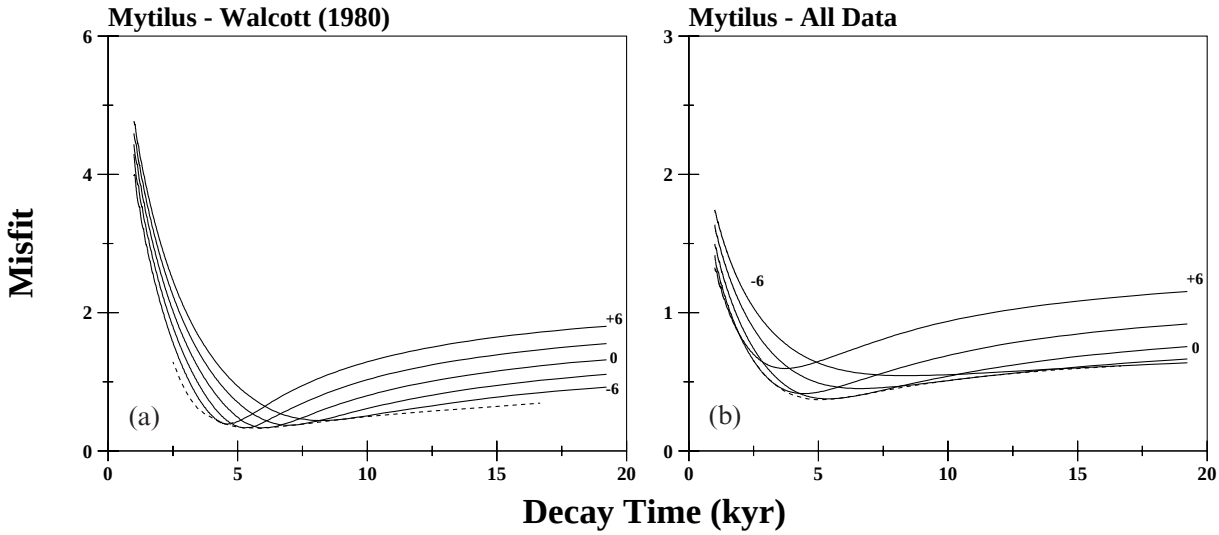

Figure 9. (a) Variation of misfit between the form (3) and the RSL constraints for Richmond Gulf adopted by Walcott (1980) (boxes in Fig. 8a) as a function of the adopted decay time. Each of the solid lines in the figure represents the best-fit curve for a specified value of the constant shift c in eq. (3) (these lines involve the values $c = -6, -3, 0, 3, 6$ m, as indicated by the small numbers on the plot). That is, these curves show the lowest misfit for a specific c, obtained by varying the RSL amplitude A (eq. 3) over a wide range as a function of the decay time. The dashed line provides the global best fit as a function of the decay time when c is varied from -10 m to 10 m in the Monte Carlo calculation. In all cases, the misfit is defined using eqs (6)–(7). (b) As in (a) except the analysis is performed on the RSL constraints given by the boxes in Fig. 8(b).

do marginally better at the shortest decay times, while lower values do somewhat better at very high (above 8 kyr) decay times. The global minimum misfit is achieved for a decay time of 5 kyr (this is $\sim$0.6 kyr lower than the global minimum case in Fig. 9a); the misfit region within 10 per cent of this global minimum defines the decay time range 4.0–6.6 kyr. The RSL curves associated with each extreme of this range are shown by the dashed ($\tau = 6.6$ kyr) and dotted ($\tau = 4.0$ kyr) lines in Fig. 8(b). Misfits within 20 per cent of the global minimum are obtained by decay times in the range 3.6–7.8 kyr; this suggests, once again, that the lower bound of the decay time is more strongly constrained by RSL data from Richmond Gulf than the upper bound.

We believe, following Walcott (1980), that a decay time estimate based on an RSL history constrained by a heterogeneous mix of samples would be less robust than the result in Fig. 9(b). As an example of such an estimate, we have repeated our analysis procedure using all the data within the Richmond Gulf region of Fig. 1 that were adopted by Peltier (1998) in his estimate of a single decay time for the entire southeastern Hudson Bay region (James Bay plus Richmond Gulf data). This analysis is reviewed in Figs 10 and 11.

A comparison of Fig. 10 and Fig. 8 indicates that the non-Mytilus edulis samples now included in the analysis are clustered within the very youngest (less than 1 kyr) portion of the sea-level history. These data consist almost exclusively of driftwood samples (see Table 1) and they tend to be displaced upwards relative to the trends established by the remaining data (see Fig. 10). Furthermore, as discussed above, Peltier (1998) excluded the Mytilus edulis sample GSC-2470 found at an elevation of 0.0 (notice that the data point on the origin of Fig. 8b is missing from Fig. 10). Both these choices effectively act to constrain the misfit analysis towards higher values of the parameter c (that is, model curves that pass above the origin at $t = 0$) and, as a consequence, the global best-fit decay time decreases (relative to the case in Fig. 9b) almost 1 kyr to

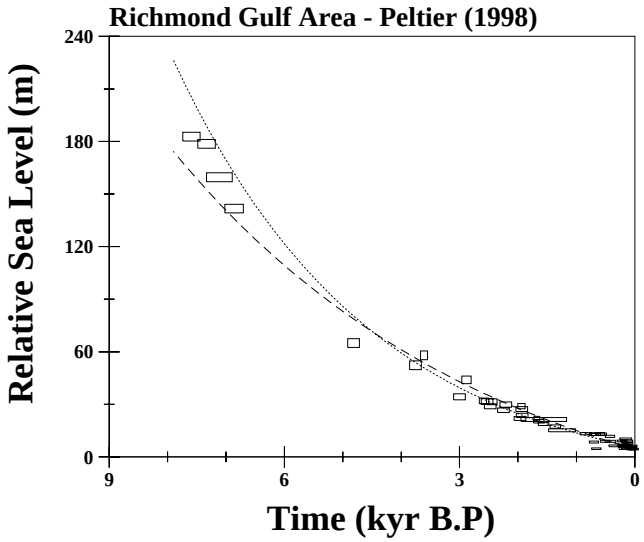

Figure 10. Collection of RSL data from Table 1 within the region defined by the Richmond Gulf inset of Fig. 1 that were adopted by Peltier (1998) in his study of RSL trends in southeastern Hudson Bay. The dashed and dotted lines represent curves of the form (3) with parameters ($A = 53$ m, $\tau = 5.5$ kyr and $c = 4.5$ m) and ($A = 24$ m, $\tau = 3.4$ kyr and $c = 5.5$ m), respectively.

4.2 kyr. A misfit tolerance 10 per cent higher than the global minimum defines the decay time range 3.4–5.5 kyr.

This exercise illustrates an important limitation of the form (3) as a model for observationally inferred sea-level histories. As the above quotations from Walcott (1980) emphasize, the shift c in this form (3) is intended to embody the deposition characteristics of a single type of sample. Driftwood samples, as their name implies, have a tendency for upward displacement from true sea level that is different from the case of, say, Mytilus edulis shells. Accordingly, searching for a single

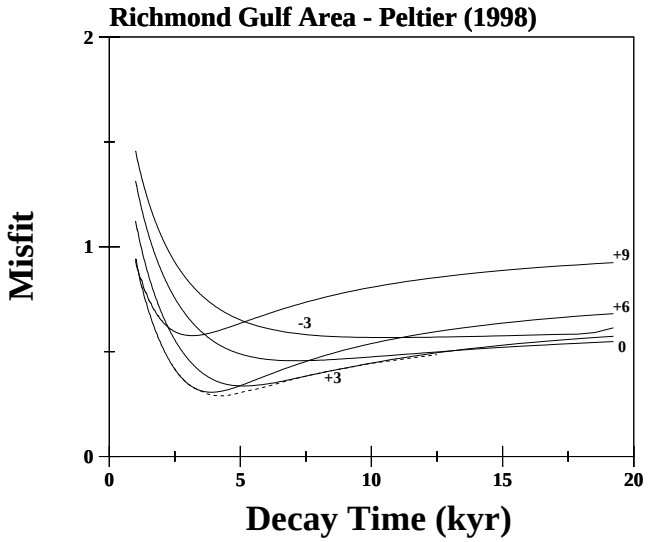

Figure 11. Variation of misfit between the form (3) and the RSL constraints shown by the boxes in Fig. 10. Each of the solid lines in the figure represents the best-fit curve for a specified value of the constant shift c in eq. (3) (these lines involve the values $c = -3$, 0, 3, 6, 9 m, as indicated by the small numbers on the plot). The dashed line provides the global best fit as a function of the decay time when c is varied from -10 m to 10 m in the Monte Carlo calculation. In all cases, the misfit is defined using eqs (6)–(7).

best-fitting form (3) through a composite RSL curve constructed from a mixed set of samples adds significant bias into the estimation procedure.

Next we turn to the RSL record within the James Bay inset of Fig. 1. In Fig. 12(a) we show data chosen by Hardy (1976) to define his uplift curve for the region (see Table 1). These data consist exclusively of shell samples. Furthermore, the dash-dotted line in Fig. 13 shows the minimum misfit, as a function of the decay time, determined from our Monte Carlo misfit analysis of this uplift curve. The misfit passes through a global minimum value for a decay time of ~ 2.5 kyr; the misfit increases dramatically for decay times longer than this value and is relatively flat for shorter decay times (at least for the range considered in Fig. 13). The misfit is within 10 per cent of the global minimum for decay times in the range 2.0–2.8 kyr. The constraint is well illustrated by the exponential forms shown in Fig. 12(a), which provide the best-fit cases for decay times near both ends of this bound. We note that the upper bound of this range increases only moderately, to 2.95 kyr, if one accepts a misfit within 20 per cent of the global minimum. It is clear that the Hardy (1976) data imply a relatively strict upper bound on the postglacial decay time of ~ 3 kyr. The shape of the minimum misfit curve (dash-dotted line) is connected both to the trend associated with the oldest data on the left frame of Fig. 12 and to the constraints related to the samples Qu-121 (sidereal age of ~ 4.5 kyr), Qu-256 and Qu-119 (with sidereal ages slightly less than and greater than 6 kyr, respectively).

Mitrovica & Peltier (1995) used Hardy's (1976) data to infer a decay time in the range 1.4–1.8 kyr. The Mitrovica & Peltier (1995) analysis only considers data within a time window extending over the last 6 kyr in C14 time or ~ 7 kyr sidereal time, the primary reason for the difference between their inference and our current best estimate.

In Fig. 12(b) we show the uplift curve adopted by Peltier (1998) for the decay time of the James Bay region. In constructing this plot we have used the error bars as they appeared in the Peltier (1998) recompilation, rather than those cited by Hardy (1976) (which we adopted in our Table 1), and this accounts for some of the differences between the two frames in Fig. 12. The most important differences between these plots, however, are the exclusion of Qu-121 in the Peltier (1998) analysis (this datum appears in his Table 1, but it is not used to

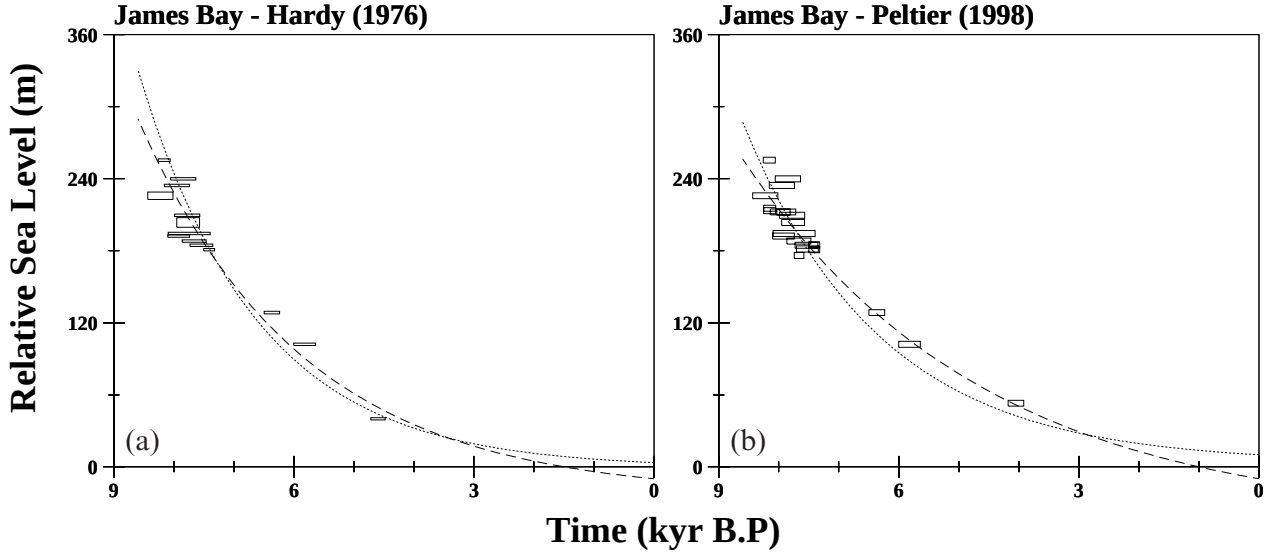

Figure 12. (a) Collection of RSL data adopted by Hardy (1976) to establish an emergence curve for James Bay. These data include all samples labelled (1976; #Y) in Table 1 with the exception of Qu-122 and Qu-124 [whose heights appear to be corrected in excess of 100 m by Hardy (1976)]. The dashed and dotted lines represent curves of the form (3) with parameters ($A = 13.75$ m, $\tau = 2.75$ kyr and $c = -10.0$ m) and ($A = 4.5$ m, $\tau = 2.0$ kyr and $c = 3.5$ m), respectively. (b) Collection of RSL data from James Bay used by Peltier (1998) to estimate a postglacial decay time for the region. In this plot we use the data as they appear in Peltier's (1998) Table 1 rather than in our own recompilation. Accordingly, the error bars are different from those in the left frame, which were taken from the original Hardy (1976) compilation. The dashed and dotted lines represent curves of the form (3) with parameters ($A = 35.25$ m, $\tau = 4.0$ kyr and $c = -10.0$ m) and ($A = 6.88$ m, $\tau = 2.3$ kyr and $c = 10.0$ m), respectively.

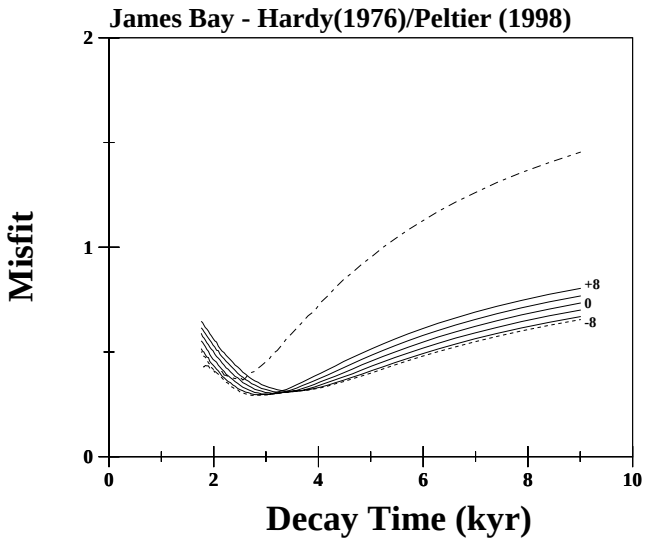

Figure 13. Solid and dashed lines: variation of misfit between the form (3) and the RSL constraints for James Bay used by Peltier (1998) (boxes in Fig. 12b) as a function of the adopted decay time. Each of the solid lines on the figure represents the best-fit curve for a specified value of the constant shift c in eq. (3) (these lines involve the values $c = -8, -4, 0, 4, 8$ m, as indicated by the small numbers on the plot). The short-dashed line provides the global best fit as a function of the decay time when c is varied from -10 m to 10 m in the Monte Carlo calculation. In all cases, the misfit is defined using eqs (6)–(7). Dash-dotted line: variation of the global best fit between the form (3) and the RSL constraints for James Bay compiled by Hardy (1976) (see Fig. 12a). To establish this line, the constant shift c is varied over the range -10 m to 10 m.

determine the decay time) and the adoption of the datum L-433A (sidereal age $\sim$4 kyr; see Table 1 and the discussion below). Since the uplift curve for James Bay has few points in the middle portion of the RSL history, the consequences of these choices on the decay time estimate are dramatic. The L-433A datum is both higher and younger than the Qu-121 sample (compare the frames of Fig. 12) and hence its inclusion (and the exclusion of Qu-121) drives the minimum misfit curves towards higher values of the decay time (see Fig. 13). Indeed, in this case the minimum misfit curve (short-dashed line in Fig. 13) is relatively flat over the decay time range $\sim$2.3–4.0 kyr, and the global minimum is obtained for a decay time of 2.8 kyr.

Peltier (1998) estimated a global best-fit decay time of 3.399 kyr for James Bay on the basis of his analysis of the data in Fig. 12(b). This value was obtained for a constant shift c (he used the symbol 'B') of 0 m. In our analysis of the data in Fig. 12(b), a value of $c = 0$ m yielded a best-fit decay time of $\sim$3.2 kyr, which is reasonably close to Peltier's (1998) estimate. The 'global' best-fit decay time depends on the range of permissible c values; however, the upper bound value of $c = 10$ m, which also appears to be the highest considered by Peltier (1998), yields a global best-fit decay time of 2.8 kyr (and an improved fit to his data relative to the $c = 0$ m case).

Qu-121 should not be excluded because it is a shell sample and thus it is consistent with all other data appearing in the Hardy (1976) database, and Hardy (1976) clearly had no reservations in regard to the datum. In fact, Hardy's (1976) inferred uplift curve was constrained to pass directly through the Qu-121 datum. Peltier (1998) apparently rejected the datum under his criteria to exclude data that were 'clearly displaced below sea level'; inspection of Fig. 12(a) suggests that this decision is questionable. Our reservations regarding the adoption of L-433A to construct the James Bay uplift curve are equally severe. First, L-433A is a driftwood sample and thus it is entirely different from all other data types (shells) that Peltier (1998) adopted for the region. Second, the datum is one of only two used by Peltier (1998) that is not derived from Hardy (1976). [The second is sample GSC-1928, which, for reasons discussed in the Appendix, we have not included in our Table 1. The L433-A sample is included in Fig. 12(b), but its inclusion or exclusion makes negligible difference to the estimated decay time.] The datum was obtained from a survey that pre-dates Hardy (1976) by several decades. Third, our search through the literature has led to the discovery of an error in the entry for this datum in the Peltier (1998) database.

Peltier (1998) incorrectly labelled the datum 'L-443A', lists a value of 53 m for the elevation (this constraint is used in Fig. 12b) and cites Lee (1962). In fact, Lee (1962) plots the datum at 57.9 m and correctly labels it as L-433A. This constraint is consistent with results in an earlier article (Lee 1960). We believe that the Peltier (1998) listing for the datum is based on Table 1 of Hillaire-Marcel (1976), where the datum is also incorrectly labelled as 'L-443A' and given an elevation of 53 m. Hillaire-Marcel (1976) referenced the datum to 'Lee in Farrand (1962)'. Farrand (1962), in turn, cited Lee *et al.* (1959) and listed an elevation of 175–190 ft (53.3–57.9 m) for L-433A. The reference Lee *et al.* (1959) lists an (approximate) elevation of 175 ft (53.3 m). Thus, while Lee *et al.* (1959) cited an elevation of $\sim$53.3 m, a series of later articles by Lee (1960, 1962) adopted an elevation of 57.9 m for the datum. This variation apparently motivated Farrand (1962) to cite the range 53.3–57.9 m for L-433A. We adopt the same range in our Table 1. Thus, Peltier's (1998) adopted elevation for L-433A (incorrectly labelled as L-443A) is actually the lower bound on the range of elevations cited for this datum. At the least, this underscores the uncertainty in elevation associated with the lone sample of driftwood.

7 FINAL REMARKS

We have presented a new compilation of RSL constraints from southeastern Hudson Bay and a detailed re-analysis of the postglacial decay times that characterize this RSL history. The latter was performed using a revised methodology for the estimation procedure that takes into account errors in both the age and height of sea-level markers, and it has been guided by results from synthetic calculations described herein. This effort has raised two main notes of caution. First, postglacial decay times estimated from relatively long RSL time-series ($\sim$9 kyr) will be biased too high unless a correction is performed for the global eustatic sea-level trend. Second, estimating a single decay time for southeastern Hudson Bay by combining RSL data from both the Richmond Gulf and James Bay regions introduces potentially large errors.

Our re-analysis of the observational data set has traced an error in previous estimates of the decay time for Richmond Gulf (e.g. Peltier 1994) to an error in the Tushingham & Peltier (1991) database of sea-level histories. Our new estimate of the decay time for this region is based, following the pioneering work of Walcott (1980), on a composite RSL curve constrained entirely by a single type of sample (in this case Mytilus edulis shells), and we infer a global best-fit decay time of 5.0 kyr. If we

choose, somewhat arbitrarily, to consider the decay times that yield minimum misfits within 10 per cent of this global minimum value, then we derive a decay time range of ~4.0–6.6 kyr. Our analysis of Hardy's (1976) data compilation for James Bay (which includes only shells) led to a best-fit decay time of 2.5 kyr (and a range, as defined above, of ~2.0–2.8 kyr).

Mitrovica & Forte (1997) adopted decay times in Hudson Bay ranging from 2.1 to 7.6 kyr in their inversions for mantle viscosity. However, their predictions, based on a best-fitting model of spherically symmetric viscoelastic relaxation, yielded values (3.3–3.8 kyr) that fell within an intermediate range of this variation. We note that these 'spherically symmetric' model predictions are also intermediate to the revised decay time ranges cited in the previous paragraph.

We question the rather precise estimates for the decay times in southeastern Hudson Bay (3.426 kyr) and James Bay (3.399 kyr) quoted in Peltier (1998) on a number of grounds. First, the adoption of a single composite sea-level curve based on data from both Richmond Gulf and James Bay is prone to large biases and acts to obscure variations evident in the individual data sets. Second, Peltier's (1998) mixing of data types (in particular simultaneously considering shells and driftwood) is not consistent with the assumptions inherent in the simple exponential form (3). Third, his data selection (both exclusions and inclusions) acts to both decrease the decay time for Richmond Gulf and increase the decay time in James Bay relative to analyses based on consistent data sets.

There is evidence in our results for a difference in the timescale of the uplift that characterizes the observational constraints from these two regions. For example, a decay time of 3.4 kyr, which falls midway between the two ranges cited above, yields a minimum misfit that is 30 per cent higher than the global minimum for the Richmond Gulf Mytilus edulis curve and 50 per cent higher than the global minimum for Hardy's (1976) uplift curve for the region (see Figs 9b and 13). We thus arrive back at Walcott's (1980) suggestion of a variation in the decay time across the Laurentide platform. It is possible that this difference simply reflects errors in the RSL data set from southeastern Hudson Bay. Alternatively, the decay times may reflect some level of lateral variation in Earth structure. This possibility is interesting given the geological evolution of Hudson Bay. Laurentia is comprised of a series of early Proterozoic orogenic belts that include a complicated mix of Archaean crust, early Proterozoic island arcs, etc. (Hoffman 1988). Superimposed on Fig. 1 we show the location of a contact between the so-called Belcher belt, a Proterozoic feature (2.0–1.8 Gyr) to the west that forms part of the Trans-Hudson Orogen, and the Superior Province, an Archaean greenstone province to the east. It is intriguing that this contact runs across the west side of Hudson Bay and effectively separates the bay from James Bay. The sensitivity of the postglacial response to the presence of such structures is worthy of future study, as is any effort to improve the quantity and quality of reliable RSL constraints for the Hudson Bay region.

ACKNOWLEDGMENTS

We thank two anonymous reviewers for their comments regarding the original manuscript. Part of this work was performed while JXM was on sabbatical leave at Caltech, and he thanks the Division of Geological and Planetary Sciences for financial support during the visit. JXM and AMF are funded, in part, from individual NSERC Operating Grants. Contribution number 8710 of the Division of Geological and Planetary Science, California Institute of Technology.

REFERENCES

Allard, M. & Tremblay, G., 1983. La dynamique littorale des iles Manitounuk durant l'Holocene, *Z. Geomorph.,* **47,** 61–95.

Andrews, J.T., 1970. *A Geomorphological Study of Postglacial Uplift With Particular Reference to Arctic Canada,* Oxford University Press, New York.

Andrews, J.T. & Falconer, G., 1969. Late glacial and post-glacial history and emergence of the Ottawa Islands, *Can. J. Earth. Sci.,* **6,** 1263–1276.

Cathles, L.M., 1975. *The Viscosity of the Earth's Mantle,* Princeton University Press, Princeton, NJ.

Craig, B.G., 1969. Late-glacial and postglacial history of the Hudson Bay region, *Earth Science Symposium on Hudson Bay*, ed. Hood, P.J., Pap. Geol. Surv. Can., **68-53,** 63–77.

Dziewonski, A.M. & Anderson, D.L., 1981. Preliminary reference Earth model (PREM), *Phys. Earth planet. Inter.,* **25,** 297–356.

Farrand, W.R., 1962. Postglacial uplift in North America, *Am. J. Sci.,* **260,** 181–199.

Forte, A.M. & Mitrovica, J.X., 1996. A new inference of mantle viscosity based on a joint inversion of post-glacial rebound data and long-wavelength geoid anomalies, *Geophys. Res. Lett.,* **23,** 1147–1150.

Hardy, L., 1976. Contribution a l'etude geomorphologique de la portion Quebecoise de la Baie de James, *PhD thesis,* McGill University, Montreal.

Hardy, L., 1977. La deglaciation et les episodes lacustre et marin sur le versant Quebecois des basses-terres de la Baie de James, *Geog. phys. Quat.,* **31,** 261–273.

Hillaire-Marcel, C., 1976. La deglaciation et le relevement isostatique a l'est de la baie Hudson, *Cah. Geogr. Que.,* **20,** 185–220.

Hillaire-Marcel, C., 1980. Multiple component postglacial emergence, *Earth Rheology, Isostasy and Eustasy,* pp. 215–230, ed. Morner, N.-A., John Wiley, New York.

Hillaire-Marcel, C. & Fairbridge, R.W., 1976. Isostasy and eustasy of Hudson Bay, *Geology,* **6,** 117–122.

Hoffman, P.F., 1988. United plates of America, *Ann. Rev. Earth planet. Sci.,* **16,** 543–603.

Kaula, W.M., 1972. Global gravity and tectonics, in *The Nature of the Solid Earth,* pp. 385–405, ed. Robertson, E.C., McGraw-Hill, New York.

Lambeck, K., 1993. Glacial rebound of the British Isles—II. A high-resolution, *Geophys. J. Int.,* **115,** 960–990.

Lambeck, K., Smither, C. & Johnston, P., 1998. Sea level change, *Geophys. J. Int.,* **134,** 102–144.

Lee, H.A., 1960. Late glacial and postglacial Hudson Bay sea episode, *Science,* **131,** 1609–1611.

Lee, H.A., 1962. Method of deglaciation, *Biul. Perygl. Lodz,* **11,** 239–245.

Lee, H.A., Eade, K.E. & Heywood, W.W., 1959. Surficial geology Sakami Lake map area, *Can. Geol. Surv. Map,* **52**.

Lowdon, J.A. & Blake, W., Jr., 1980. Radiocarbon dates XX, *Pap. Geol. Surv. Can.,* **80-7**.

Lowdon, J.A., Fyles, J.G. & Blake, W., Jr., 1967. Geological Survey of Canada radiocarbon dates VI, *Radiocarbon,* **9,** 156–197.

Mathews, B., 1966. Radiocarbon-dated postglacial land uplift in northern Ungava, *Nature,* **211,** 1164–1166.

McConnell, R.K., 1968. Viscosity of the mantle from relaxation time spectra of isostatic adjustment, *J. geophys. Res.,* **73,** 7089–7105.

Milne, G.A., Mitrovica, J.X. & Davis, J.L., 1999. Near-field hydro-isostasy: the implementation of a revised sea-level equation, *Geophys. J. Int.,* **139,** 464–482.

Mitrovica, J.X. & Forte, A.M., 1997. The radial profile of mantle viscosity: results from the joint inversion of convection and post-glacial rebound observables, *J. geophys. Res.,* **102,** 2751–2769.

Mitrovica, J.X. & Peltier, W.R., 1993. A new formalism for inferring mantle viscosity based on estimates of post-glacial decay times: application to RSL variations in N.E. Hudson Bay, *Geophys. Res. Lett.,* **20,** 2183–2186.

Mitrovica, J.X. & Peltier, W.R., 1995. Constraints on mantle viscosity based upon the inversion of postglacial uplift data from the Hudson Bay region, *Geophys. J. Int.,* **122,** 353–377.

Nakada, M. & Lambeck, K., 1989. Late Pleistocene and Holocene sea-level change in the Australian region and mantle rheology, *Geophys. J. Int.,* **96,** 497–517.

Pari, G. & Peltier, W.R., 1996. The free-air gravity constraint on subcontinental mantle dynamics, *J. geophys. Res.,* **101,** 28 105–28 132.

Peltier, W.R., 1976. Glacial isostatic adjustment, *Geophys. J. R. astr. Soc.,* **46,** 669–706.

Peltier, W.R., 1982. Dynamics of the ice age Earth, *Adv. Geophys.,* **24,** 1–146.

Peltier, W.R., 1985. Mantle convection and viscoelasticity, *Ann. Rev. Fluid Mech.,* **17,** 561–608.

Peltier, W.R., 1994. Ice age paleotopography, *Science,* **265,** 195–201.

Peltier, W.R., 1998. Postglacial variations in the level of the sea: implications for climate dynamics and solid-earth geophysics, *Rev. Geophys.,* **36,** 603–689.

Peltier, W.R. & Wu, P., 1982. Mantle phase transitions and the free air gravity anomalies over Fennoscandia and Laurentia, *Geophys. Res. Lett.,* **9,** 731–734.

Peltier, W.R, Forte, A.M., Mitrovica, J.X. & Dziewonski, A.M., 1992. Earth's gravitational field: seismic tomography resolves the enigma of the Laurentian anomaly, *Geophys. Res. Let.,* **19,** 1555–1558.

Plumet, P., 1974. L'archeologie et le relevement glacio-isostatique de la region de Poste-de-la-Baleine, *Rev. Geogr. Montr.,* **28,** 443–447.

Simons, M. & Hager, B.H., 1997. Localization of the gravity field and the signature of glacial rebound, *Nature,* **390,** 500–504.

Tushingham, A.M. & Peltier, W.R., 1991. ICE-3G: a new global model of late Pleistocene deglaciation based upon geophysical predictions of postglacial relative sea level change, *J. geophys. Res.,* **96,** 4497–4523.

Tushingham, A.M. & Peltier, W.R., 1992. Validation of the ICE-3G model of Wurm-Wisconsin deglaciation using a global data base of relative sea level histories, *J. geophys. Res.,* **97,** 3285–3304.

Walcott, R.I., 1972. Late Quaternary vertical movements in Eastern North America: quantitative evidence of glacio-isostatic rebound, *Rev. Geophys. Space Phys.,* **10,** 849–884.

Walcott, R.I., 1973. Structure of the earth from glacio-isostatic rebound, *Ann. Rev. Earth planet. Sci.,* **1,** 15–37.

Walcott, R.I., 1980. Rheological models and observational data of glacio-isostatic rebound, *Earth Rheology, Isostasy and Eustasy,* pp. 3–10, ed. Morner, N.-A., John Wiley, New York.

Walcott, R.I. & Craig, B.G., 1975. Uplift studies, *Pap. Geol. Surv. Can.,* **75-1**.

Webber, P.J., Richardson, J.W. & Andrews, J.T., 1970. Post-glacial uplift and substrate age at Cape Henrietta Maria, *Can. J. Earth Sci.,* **7,** 317–325.

Wu, P. & Peltier, W.R., 1983. Glacial isostatic adjustment and the free air gravity anomaly as a constraint on deep mantle viscosity, *Geophys. J. R. astr. Soc.,* **74,** 377–449.

APPENDIX A: NOTES ON TABLE 1

A recompilation of observational constraints on sea-level trends in southeastern Hudson Bay relies heavily on relatively few principal sources. These include Hillaire-Marcel (1976), Hardy (1976) and Allard & Tremblay (1983). Indeed, these references alone account for about 90 per cent of the recent recompilation by Peltier (1998). (For the sake of brevity, this database is denoted P98 in the discussion below.) Nevertheless, a collection of these data together is clearly a worthy exercise for future research.

There are a number of important data points not included in the P98 recompilation, and one of the purposes of Table 1 is to include these data (they are identified by a blank entry in column 5). We note that these constraints are associated primarily with the sites Poste de la Baleine, Petite Riviere de la Baleine, Manitounuk Peninsula and Cape Henrietta Maria. There are undoubtedly other data that we have missed.

Given the archival goal of the exercise, the accuracy of recompilations is important. Accordingly, we have corrected a number of errors in the P98 database. The symbol ‡ in Table 1, column 5, indicates the locations of these revisions. In brief, these are as follows. (1) The heights of GSC-1287 and GSC-1238 are corrected to reflect entries in Hillaire-Marcel (1976). (2) P98 lists the height for GIF-1567 as '30?', but both the original reference, Plumet (1974), and Hillaire-Marcel (1976) list it as 62 m. (3) The C14 age of Qu-1296 (Manitounuk Peninsula) is given as 2750 yr in P98; Allard & Tremblay (1983) list a C14 age of 2510 yr. (4) The data Qu-1209 and Qu-1087 are associated with Neilsen Island in P98 but they are located in Merry Island (Allard & Tremblay 1983). (5) Datum Qu-1067 is incorrectly cited as Qu-1007 in P98. (6) The site Bill of Portland is listed as Bill of Portugal in P98. (7) The height of Qu-1091 is corrected to 7.0 m. (8) P98 lists a height of 53 m for sample L-443A with reference to Lee (1962). The datum label is incorrect (it should read L-433A) and the height adopted by P98 is suspect. See text for a detailed discussion of this datum and our revised entry. (9) The height of Qu-256 is corrected to 100 m. (10) Datum Qu-255 is incorrectly cited as Qu-172 in P98. (11) Labels Qu-122 and Qu-124 are incorrectly switched in P98. Furthermore, P98 does not list the elevation corrections adopted by Hardy (1976). (12) Qu-252 is referenced to Vincent in P98, but Hardy's (1976) compilation does not support this. (13) The age of sample GSC-2161 is corrected to 7110 yr. Finally, the age of sample GSC-2070 is given as 3360 yr in our table. This age is consistent with information in Walcott & Craig (1975). In contrast, P98, following Walcott (1980), cited an age of 3330 yr. The origin of this discrepancy is unclear.

We have revised some references in order to reflect the oldest citation found for a particular datum. We have also omitted three data points appearing in P98, GSC-1959 (elevation 178 m), GSC-2135 (elevation 205 m) and GSC-1928, because we were unable to find any reference to them (although they probably exist in sources unavailable to us) as well as data from Povungnituk on the grounds that the site is not in southern Hudson Bay (see Fig. 1). In the final footnote to P98's Table 1, the datum Qu-1959 is described as 'a replicate measurement at the same site' as Qu-256, and the former is then treated as suspect. This is an error. Qu-120 and Qu-256 are replicate measurements and we drop the former.